Received: 10 July 2020 | Revised: 16 February 2021 | Accepted: 11 May 2021

DOI: 10.1111/mec.15984

ORIGINAL ARTICLE

MOLECULAR ECOLOGY WILEY

# Quality of phytoplankton deposition structures bacterial communities at the water-sediment interface

Dandan Izabel-Shen[1] | Séréna Albert[1] | Monika Winder[1] | Hanna Farnelid[2] | Francisco J. A. Nascimento[1]

[1]Department of Ecology, Environment and Plant Sciences, Stockholm University, Stockholm, Sweden

[2]Center for Ecology and Evolution in Microbial Model Systems, Linnaeus University, Kalmar, Sweden

**Correspondence**
Dandan Izabel-Shen, Department of Ecology, Environment and Plant Sciences, Stockholm University, Stockholm, Sweden.
Email: dand.shen@gmail.com

**Funding information**
Swedish Environmental Protection Agency's Research, Grant/Award Number: NV-802-0151-18; Swedish Research Council Formas, Grant/Award Number: Grant no. 2015-1320 and 2016-00804

## Abstract

Phytoplankton comprises a large fraction of the vertical carbon flux to deep water via the sinking of particulate organic matter (POM). However, despite the importance of phytoplankton in the coupling of benthic-pelagic productivity, the extent to which its deposition in the sediment affects bacterial dynamics at the water-sediment interface is poorly understood. Here, we conducted a microcosm experiment in which varying mixtures of diatom and cyanobacteria, representing phytoplankton-derived POM of differing quality, served as inputs to sediment cores. Characterization of *16S rRNA* gene of the bacterial communities at the water-sediment interface showed that bacterial α-diversity was not affected by POM addition, while bacterial β-diversity changed significantly along the POM quality gradient, with the variation driven by changes in relative abundance rather than in taxon replacement. Analysing individual taxa abundances across the POM gradient revealed two distinct bacterial responses, in which taxa within either diatom- or cyanobacteria-favoured groups were more phylogenetically closely related to one another than other taxa found in the water. Moreover, there was little overlap in taxon identity between sediment and water communities, suggesting the minor role played by sediment bacteria in influencing the observed changes in bacterial communities in the overlying water. Together, these results showed that variability in phytoplankton-originated POM can impact bacterial dynamics at the water-sediment interface. Our findings highlight the importance of considering the potential interactions between phytoplankton and bacteria in benthic-pelagic coupling in efforts to understand the structure and function of bacterial communities under a changing climate.

KEYWORDS
bacteria, particulate organic matter, phytoplankton blooms, The Baltic Sea, water-sediment interface

Dandan Izabel-Shen and Séréna Albert contributed equally to this work.

## 1 | INTRODUCTION

The sedimentation of phytoplankton is a major pathway driving benthic-pelagic coupling (Griffiths et al., 2017), as the sinking particulate organic matter (POM) results in the export of carbon and nitrogen through the oceanic water column down to the sea floor (Burd & Jackson, 2009; Farnelid et al., 2019; Mestre et al., 2018; Zinger et al., 2011). Inputs of this POM source to the deeper water and sediments account for a major proportion of the organic material that fuels food webs and biogeochemical cycles in benthic systems (Griffiths et al., 2017). In addition, the dissolved organic matter (DOM) released into the water column by phytoplankton, whether by direct excretion or by trophic interactions, can be readily taken up by heterotrophic bacteria to produce living biomass (Azam et al., 1994). Changes in phytoplankton composition alter the quantity and quality of organic matter (OM) pools, and therefore the composition of the associated microbial communities in the surface and bottom waters (Amon & Benner, 1996; Ye et al., 2011).

Phytoplankton blooms develop throughout the year and differ in terms of their species composition. For example, in temperate coastal systems, spring blooms are often dominated by diatoms and/or dinoflagellates and summer blooms by cyanobacteria (Hoikkala et al., 2016; Larsson et al., 2001; Lindh et al., 2015). The bacterial assemblages associated with phytoplankton blooms are usually phylogenetically diverse (Landa et al., 2018; Lindh et al., 2015; Nowinski et al., 2019). In addition, empirical data obtained from ocean or freshwater habitats (Finn et al., 2017; Nelson & Carlson, 2012) and experiments (Landa et al., 2014) have shown that the succession of bacterial communities is related to the variability of phytoplankton biomass and species identity in pelagic zones as well as in sediments (Franco et al., 2007). However, none of them examined whether and how living phytoplankton after reaching the sediment surface impact the bacterial assemblages at the water-sediment interface.

The composition and coexistence of the heterotrophic bacterial assemblages that make use of phytoplankton-derived OM are determined by resource availability (quantity) and resource composition (quality) (Kirchman, 2003; Mühlenbruch et al., 2018). Both field investigations (Repeta et al., 2002; Romera-Castillo et al., 2013) and experimental studies have shown that phytoplankton releases different types of inorganic and organic molecules, depending on the producing species (Fu et al., 2020; Kirchman, 2003). Phytoplankton-derived DOM and POM differ in their lability (Mühlenbruch et al., 2018; Wu et al., 2003) and therefore in their accessibility within the microbial loop. Several studies have focused on how changes in OM quantity and concentration alter the diversity and composition of the bacterial community (Eiler et al., 2003; Needham & Fuhrman, 2016; Pinhassi & Berman, 2003), yet information on the effect of OM quality on bacterial community structure is scarce. Changes in OM quality have been shown to impact microbial activity and dynamics in some systems (Crump et al., 2017; Smith et al., 2018), but not in others (Sarmento et al., 2016).

Although distribution and composition of bacterial communities can differ substantially between sediments and overlying open waters, their dynamics are often coupled, and contribute to biogeochemical interconnections between the pelagic and the benthic habitats (Dang & Lovell, 2016; Zinger et al., 2011). The breakdown of OM and nutrient regeneration mediated by sediment bacteria might in turn influence the microbial community composition and abundance in overlying water (Dang & Lovell, 2016). Furthermore, the proportion of dormant bacterial cells in sediments is estimated to be 30% (Jones & Lennon, 2010); 26%–42% of those cells can potentially be reactivated, with their growth triggered by nutrient enrichment (Luna et al., 2002). The low-abundance taxa from seed banks can contribute disproportionally to the overall community dynamics (Shade et al., 2014). Hence, assessing the extent to which sediment bacteria contribute to the dynamics of overlying water communities can provide insights into the potential for competition and niche partitioning among coexisting bacteria responsible for OM degradation in the water-sediment interface.

Unlike other estuaries, the long water residence time and landlocked shelf-sea system of the Baltic Sea (Reissmann et al., 2009) make it more susceptible to the impacts of climate change and anthropogenic activities. The Baltic Sea has been subjected to eutrophication progressively, which has been projected to favour the predominance of cyanobacteria over diatoms in the water column and thus in the composition of bloom-forming phytoplankton (Griffiths et al., 2017). The importance of benthic-pelagic coupling for Baltic Sea ecosystem functioning under shifting environmental conditions has been discussed at length (Griffiths et al., 2017). From the perspective of benthic organisms, cyanobacteria are poor sources of fatty acids, amino acids and are thus a nutritionally less favourable food source for macro- and meiofauna consumers than diatoms (Brown, 1991; Nascimento et al., 2009). Accordingly, a large amount of the OM originating from unconsumed cyanobacteria would have the potential to enhance the microbially-mediated decomposition of OM. The diatom *Skeletonema marinoi* and cyanobacteria *Nodularia spumigena* are major participants in the spring and summer blooms of phytoplankton, respectively, in the central Baltic Sea (Wasmund et al., 2011). Here, we conducted a microcosm experiment in which *S. marinoi* and *N. spumigena* were mixed in varying proportions to simulate a POM quality gradient, and then added as OM inputs to the sediment. Our goal was to examine the impact of heterogeneous decomposition of phytoplankton-originated POM on bacterial communities at the water-sediment interface. We hypothesized that: (i) settling POM alters the diversity and composition of bacterioplankton assemblages, (ii) changes in community composition along a POM quality gradient will lead to a higher proportion of taxa associated with high cyanobacterial supply versus those associated with diatom supply, and (iii) recruitment from sediment communities contribute to the response of overlying water bacterial assemblages to POM mixtures.

## 2 | MATERIALS AND METHODS

### 2.1 | Study site and sampling

Sediments were obtained on 4 September 2017 from Hållsviken, in the northern Baltic Sea proper (58°50′ N, 17°31′ E), at 27 m water depth using a box-corer (0.2 $m^2$). All sediment cores were collected in close proximity to attempt similar initial community composition in the water and sediments. The collected sediments were subsampled onboard using acrylic corers (30 × 4.6 cm, 17 $cm^2$ surface area) and were handled carefully to limit disturbance of the water-sediment interface. The sediment cores were capped with rubber plugs and brought to the Askö Marine Research Station, located near the sampling site.

### 2.2 | Experimental design

Before starting the experiment, the water in each core was almost entirely removed, until ~1 cm of overlying water remained. Water collected in the vicinity of the sampling site at Askö Marine Research Station was filtered through 0.22 μm membranes (Millipore) to remove the majority of microorganisms and organic matter aggregates, and gently added to each experimental unit. Each core consisted of 10 cm of sediment and 20 cm (330 ml) of overlying water. This set-up allowed for characterizing the bacterial communities in the water overlying sediment, while minimizing differences in species pools of starting communities, and preserving the sediment in situ conditions for each core. Each core was aerated with a thin silicon tube inlet (approximately 20 cm in length × 2 mm in diameter), connected to a central air pump to ensure constant oxygenation of the overlying water. All cores were kept in a constant-temperature room at the in situ temperature (4.5 ± 1°C) with a light intensity of 0.4 $\mu E/m^2/s$ and a day/night light cycle (15:9 h) for 14 days, sufficient to allow the microbes to acclimate to the experimental conditions.

The diatom and cyanobacteria cultures chosen as OM sources were *S. marinoi* (strain LYS6AAF, provided by the Department of Environmental Science and Analytical Chemistry, Stockholm University) and *N. spumigena* (strain K-1537, provided by the Norwegian Institute for Water Research, Norway), respectively. The same medium ("Stock culture" described in Karlsson & Winder, 2018) was used in the two cultures, with additional $Na_2SiO_4$ supplemented for *S. marinoi*. The cultures were grown at 15°C, under a 16:8 h day/night cycle and salinity 23 for *S. marinoi* and 11 for *N. spumigena*. After 6 days of culture, *N. spumigena* was concentrated by sieving and *S. marinoi* by centrifugation. The cells of each strain were collected in separate tubes and rinsed three times with sterile artificial seawater. During the concentration process, the salinity of the water was gradually brought to salinity 15 (*S. marinoi*) and salinity 6 (*N. spumigena*), thus approaching the in situ salinity conditions while preserving the integrity of the cells (checked visually under a microscope).

Organic matter was derived from diatom and cyanobacteria slurries (~500 ml each) and its ash-free dry weight (AFDW) was determined by high-temperature combustion. For each phytoplankton slurry, five 1 ml replicates were pipetted onto precombusted (4 h at 500°C) and weighed GF/F filters (Whatman), dried at 60°C for 24 h, and then combusted for 4 h at 500°C. The filters were weighed after each step using a microbalance (Sartorius M3P, precision ± 0.001 mg) and their OM concentrations calculated as mg AFDW/L. The remaining volumes of the slurries were kept at 10°C in the dark until the start of the experiment (c. 1 week).

One day prior to the start of the experiment, the cyanobacteria's gas vacuoles were collapsed by applying a sudden pressure shock (Nascimento et al., 2008), which caused the organisms to settle to the sediment surface. The diatom and cyanobacteria slurries were homogenized and then added by pipetting evenly at the surface of each sediment core, during which time the airflow device was stopped. A POM quality gradient comprising approximately equal amounts (dry weight) of OM, standardized to ~2 mg AFDW/$m^2$ but varying in the proportions of diatom (D) and cyanobacteria (C) slurries, was added to the sediment cores as follows (Figure 1): 100% diatom (100D), 80% diatom/20% cyanobacteria (80D_20C), 50% diatom/50% cyanobacteria (50D_50C), 20% diatom/80% cyanobacteria (20C_80D) and 100% cyanobacteria (100C). An additional set of cores without POM addition served as the controls. The experimental setup thus consisted of six treatments, each with five replicates (Figure 1), for a total of 30 replicate microcosms. Most of the added POM settled onto the sediment surface of all microcosms within 12 h, but some cyanobacterial filaments floated at the water surface. These buoyant filaments were carefully removed from each core, mixed with 2 g of 500 μm-sieved sediment from the study site, and spread evenly on the surface of the sediment from the corresponding core. However, to maintain the same level of physical disturbance in all microcosms, the controls and 100D were subjected to the same action: for the respective sediment cores, mixing the overlying water with the presieved sediment, and distributing evenly to the surface of the sediment. The microcosms were then covered with parafilm and aeration was restarted. The experiment lasted for 24 days under the temperature and light conditions described above.

### 2.3 | Water chemical analyses

After OM addition, water samples were taken from all microcosms at the beginning (day 0) and end of the experiment (day 24) for the determination of $NH_4^+$, $PO_4^{3-}$ and NOx (integrated forms of $NO_2^-$ and $NO_3^-$). For each sample, 15 ml of water was filtered through a polyethersulphone syringe filter with a 0.2 μm pore-size (Whatman) and kept at −20°C until further analysis. Inorganic nutrient concentrations were measured on a segmented flow nutrient analyser system (OI Analytical, Flow Solution IV). Table S1 summarizes the results of the chemical and biological measurements of the water samples.

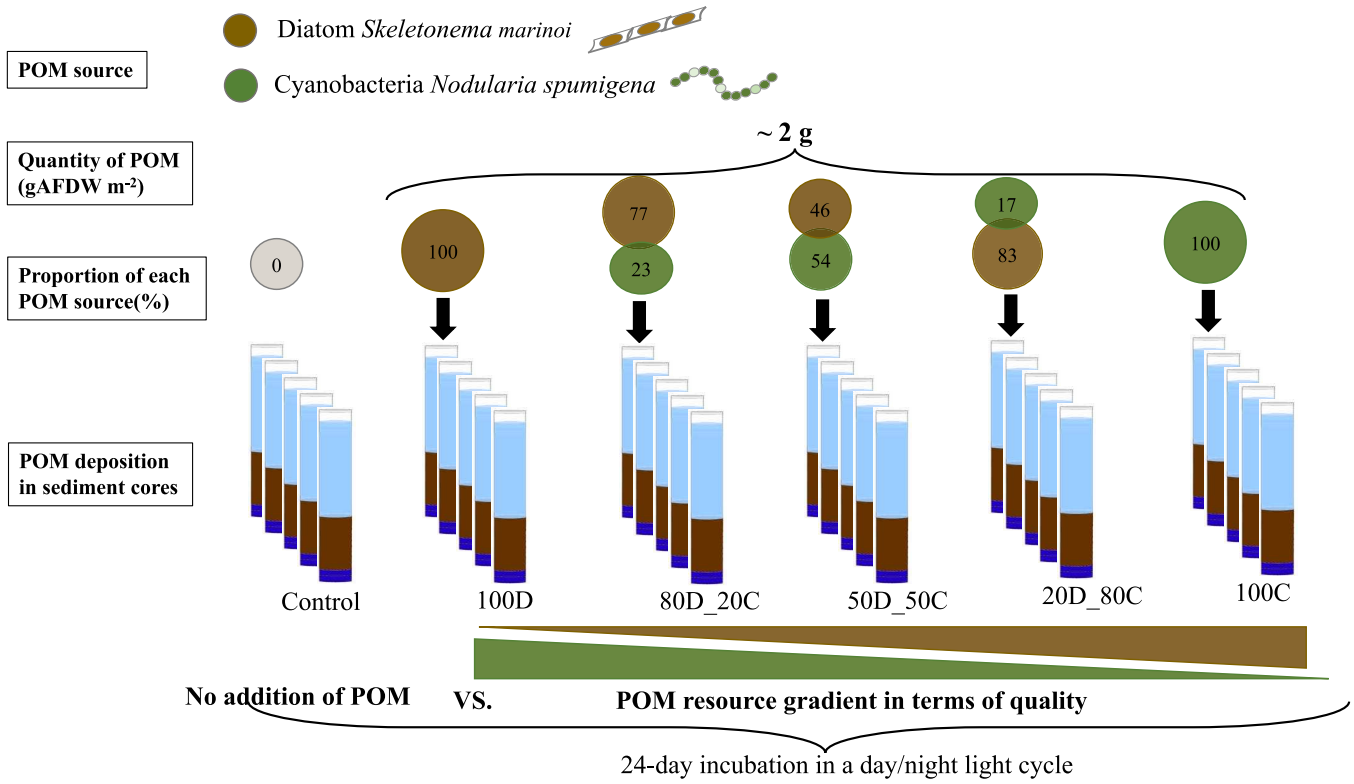


FIGURE 1 Experimental setup. Particulate organic matter (POM) gradients differing in their diatom (D) and cyanobacteria (C) contributions (%) were established as follows: 100D, 80D_20C, 50D_50C, 20D_80C, 100C, respectively. Control microcosms contained no added POM. For each sediment core, the water phase of the microcosms is indicated in light blue, the sediment phase in brown, and the closure in dark blue

## 2.4 | Bacterial abundance

Bacterial cell abundances in all microcosms were determined on day 7 and at the end of the experiment using flow cytometry as described elsewhere (Gasol & del Giorgio, 2000). Briefly, 1.6 ml of water was sampled from each core, approximately 5 cm below the water surface. Samples were preserved with glutaraldehyde at a final concentration of 1% and immediately flash-frozen in liquid nitrogen until the analysis. Cells in the samples were stained using SYBR Green I and then enumerated using a Cube8 flow cytometer (CyFlow space). An example cytogram showing the applied gating for counting bacterial cells is displayed in Figure S1.

## 2.5 | Nucleic acid extraction and sequencing

Nucleic acids were sampled from the slurries (10 ml, $n$ = 3) on day 0, and all water from each core (~300 ml, $n$ = 29) on day 24 of the experiment, and were filtered onto 47 mm diameter, 0.2 µm pore size Supor membrane filters (Pall Corporation). One replicate of the "100D" treatments was not included in DNA extraction due to water loss during sampling. The filters were placed in 2 ml cryovials, flash frozen with liquid nitrogen and stored at −80°C until used for nucleic acid extraction. DNA from the 32 samples was extracted using the FastDNA spin kit for soil (MP Biomedicals), optimized for marine phytoplankton samples, according to the manufacturer's instructions with minor modifications.

The sediment communities of the microcosms were characterized to assess the extent to which bacterial populations in the sediments influenced the response of bacterioplankton inhabiting the overlying water to the POM inputs. Hence, the top 3 cm of the sediment from the initial cores (day 0) and from each microcosm at the end of the experiment (day 24) were sliced, immediately flash-frozen with liquid nitrogen and stored at −80°C until nucleic acid extraction. The RNA from 35 samples was extracted using the RNeasy PowerSoil kit (Qiagen) according to the manufacturer's protocol. Genomic DNA in the RNA extracts was removed by DNase treatment using the TURBO DNA-free kit (Invitrogen). The DNase-treated RNAs were tested for traces of genomic DNA by PCR amplification. Finally, the RNA extracts were reverse transcribed using the AccuScript High Fidelity first strand cDNA synthesis kit (Agilent Technologies). Both the metabolically active fraction of the sediment communities (RNA-based) and the total communities in the overlying water (DNA-based) were determined. This approach allowed an assessment of the contribution of active bacteria in the sediment to the community dynamics of the sediment-water interface. For all samples (DNA-based and RNA-based), the hypervariable region of 16S bacterial V3–V4 was targeted using primers 341f/805r (Herlemann et al., 2011) and then sequenced using the Illumina MiSeq system (2 × 300 based pairs) at SciLifeLab, Stockholm. All molecular work

was conducted in dedicated laboratory benches, regularly cleaned with 70% ethanol and equipped with UV-chambers, and laboratory supplies were autoclaved and cleaned with 10% sodium hypochlorite solution prior to being placed on the bench. Ultraclean molecular grade-water was used for PCR negative controls, which were pooled and sequenced alongside the biological samples. High levels of biological replications in our experimental setup allowed us to control inherent biases from nucleic extraction, PCR and sequencing and to make reliable ecological conclusions (Zinger et al., 2019).

## 2.6 | Sequence processing

Raw sequences were processed using the DADA2 pipeline (Callahan et al., 2017) according to the DADA2 tutorial (v.1.12) in R. The sequences were quality filtered with customized modifications as follows: truncLen = c(280,220), maxEE = 2, truncQ = 2, maxN = 0, rm.phix = TRUE, trimLeft = c(10,10). Subsequently, denoising, merging and chimera removal were completed according to the DADA2 pipeline tutorial. The filtered FASTQ files were dereplicated and unique sequences with their corresponding number of reads were assigned as amplicon sequence variants (ASVs). All sequences were aligned and assigned taxonomically using the SILVA v.132 reference database (Quast et al., 2013). All archaea, eukaryote, mitochondria, and chloroplast sequences were removed. Singletons (ASVs with only one sequence read across all samples) were also discarded. A total of 113 reads were found in the negative control, which belonged to the two most abundant ASVs found in the data set (https://github.com/IzabelShen/PAPER_IzabelShen_AlgaPOM_2021/blob/main/ASV_table_before_normalization.xlsx). These sequences most probably correspond to internal contaminants introduced during the sequencing (Mitra et al., 2015). They were therefore not filtered out from the data set to avoid losing biologically relevant information (Taberlet et al., 2018).

Amplicon sequence variants detected in the phytoplankton slurries and microcosms with POM addition, but not in the controls or in the initial sediment communities, were filtered out from the water and sediment data sets, to ensure that potential changes in bacterial communities in response to POM addition were not the bacterial associates added with the phytoplankton slurries upon initiation of the experiment (Figure S2). The removed AVSs collectively represented <0.03% of those in the POM-treated communities and are referred to as "Uniq_Slu%" in Table S2. To standardize the sequencing effort, the ASV tables derived from the water and sediment data sets were rarefied to their respective smallest library size (187,434 and 14,712 respectively) and found to contain 3692 and 6570 unique ASVs in the respective data sets (see Table S2 for details).

## 2.7 | Statistical analyses

A repeated-measurement ANOVA was used to test the effects of time, POM addition, and their interaction on total cell numbers and the concentrations of inorganic nutrients. In the case of significant effects of time, a one-way ANOVA was carried out to separately explore the differences in cell abundance and nutrients for each time point. To assure fulfillment of the assumptions of the ANOVA, the normal distribution of the residuals of the linear models was tested using the Shapiro–Wilk normality test in the STATS package (v.3.6.2). The homogeneity of variance was tested using Levene's test from the CAR package (v.3.0.6). The data were log-transformed when necessary to fulfill the ANOVA requirements.

Within-sample (α)-diversity was estimated by computing the richness from the normalized counts, with 100 iterations, using the VEGAN R package (v.2.5.6). Evenness was calculated as the quotient of the Shannon diversity/the natural logarithm (ln) of the richness. A one-way ANOVA was used to analyse the effect of phytoplankton POM deposition on α-diversity among treatments. To explore the taxonomic and phylogenetic patterns giving rise to β-diversity, the community dissimilarity among treatments was calculated based on the Bray–Curtis distance (Bray & Curtis, 1957) as well as the weighted and unweighted UniFrac matrices (Lozupone & Knight, 2005); the results were visualized using nonmetric multidimensional scaling (NMDS). The resemblances generated from both Bray–Curtis and UniFrac distance matrices helped assess whether both phylogenetic breadth and the relative abundance of taxa are important to interpret the responses of overall community to POM mixtures. The robustness of resemblance patterns was further tested using pairwise Mantel tests. Potential effects of POM addition on bacterial community composition in the water column were analysed using permutational multivariate analyses of variance (PERMANOVA) (Anderson, 2001). PERMANOVA tests were performed separately for each of the three dissimilarity matrices. All the above-mentioned data analyses were performed using the VEGAN package (Oksanen et al., 2011).

To identify individual bacterial responses to POM addition, each ASV was screened for an increase or decrease in relative abundance between treatments with high diatom addition (i.e., 100D and 80D_20C) versus high cyanobacteria addition (i.e., 100C and 20D_80C) using the DESEQ2 R package (v.1.26.0). Significant values were corrected for multiple tests using the Benjamini–Hochberg procedure with an adjusted α value of 0.2. ASVs that passed this significant filtering in the differential abundance analysis were considered representative of bacteria with a distinct phytoplankton-originated POM preference and enriched by the addition of either high diatom- or cyanobacteria-derived OM (referred to hereafter as "diatom-favoured" and "cyano-favoured" taxa, respectively). To check the robustness of the differential abundances against the microcosms containing equal proportions of diatom and cyanobacteria (50D_50C), the occurrence patterns of the ASVs were explored using a hierarchical analysis with Pearson's correlation. ASVs with similar relative abundance patterns across the varying POM quality gradient were grouped with a dendrogram without any information on their phylogeny. A heatmap with colour gradients was used to display the trend in the relative abundance of each ASV. An analysis of similarity (ANOSIM) was used to test whether the groupings of the two clusters differed significantly from one another.

In addition, the net relatedness index (NRI) and the nearest taxon index (NTI) were applied to test whether the ASVs in an ecological category (either diatom-favoured or cyanobacteria-favoured) were more phylogenetically closely related to one another, than other ASVs found in the water. The former is a measure of the mean phylogenetic distance between all pairs drawn from a community, and the latter calculates the mean phylogenetic distance between all individuals and their closest relatives (Webb et al., 2002). Both NRI and NTI metrics were then used to test the relatedness of the ASVs within each group and how presence/absence relates to POM preference. This was done using the PICANTE package (v.1.8.1; Kembel et al., 2010) with R. Additionally, a local bacterial pool was constructed by using all 3692 ASVs to investigate whether the phylogenetic clustering differed from a random clustering. A phylogenetic tree of all ASVs was constructed using MAFFT (Katoh et al., 2002) and FASTTREE (Price et al., 2009) implemented in QIIME2 (v.2019.10). The observed NRI or NTI was then compared with a null distribution of 1000 communities drawn at random from the local pool selected by shuffling the ASV labels. According to Stegen et al. (2012), NRI or NTI greater than +2 indicates that coexisting taxa within a community are more closely related than expected by chance, namely, phylogenetic clustering. NRI or NTI less than −2 indicates that coexisting taxa are more distantly related than expected by chance, namely, phylogenetic overdispersion. The values falling within −2 and +2 indicate that coexisting taxa within a community undergo stochasticity. The phylogenies of the significantly enriched ASVs were visualized using ITOL v.5 (Letunic & Bork, 2019).

Finally, to assess whether taxon enrichment was associated with inorganic nutrients, the correlations between the $NH_4^+$, $PO_4^{3-}$ and NOx concentrations and the relative abundance of significantly enriched taxa were analysed using Spearman rank correlation analyses. A rho coefficient <0 indicates a negative correlation, and a rho coefficient >0 a positive correlation.

## 3 | RESULTS

### 3.1 | Experimental conditions and bacterial abundance

The concentrations of both $NH_4^+$ and $PO_4^{3-}$ were similar across treatments at each time point (Figures S3A,B; Table S1), but NOx fluctuated among the POM-added treatments (Figure S3C). The time effect was significant for all measured inorganic nutrients in all treatments: $NH_4^+$ progressively decreased during the experiment whereas $PO_4^{3-}$ and NOx increased significantly (repeated-measurement ANOVA, time effect: $p < .001$). The correlations between NOx and $PO_4^{3-}$ concentrations were significantly positive (Pearson's $R = .52$, $p = .004$; Figure S3D), but the correlation between NOx and $NH_4^+$ was weak and not significant ($R = .16$, $p = .41$).

Bacterial abundances differed over time (Figure S4; repeated-measurement ANOVA, time effect: $p < .001$). On day 7, the cell counts were significantly lower in the controls ($0.38 \pm 0.10 \times 10^5$ cells/ml) than in the POM treatments ($2.77–5.25 \times 10^5$ cells/ml), with the exception of 100D (Figure S4; ANOVA, $p < .001$). This difference in cell abundances between the controls and most POM treatments persisted also at the end of the experiment (day 24) ($p < .01$), despite the significant bacterial growth in all treatments compared to day 7. The absence of a strong correlation between bacterial abundance and inorganic nutrient concentrations suggested that nutrient availability was not the limiting factor for bacterial growth over time in our experiment.

### 3.2 | Minimal overlap in taxon identity between sediment and water communities

The overlap of bacterial ASVs across sediment and water samples was determined in order to investigate the response of the communities in the overlying water to POM addition as a function of the recruitment from sediment bacteria. Of the 6570 sediment and 3692 water ASVs, 547 were present in both pools (Venn diagram, Figure 2a). In terms of relative abundance, the shared ASVs made up 11%–50.94% of individual sediment communities and 73.32%–79.88% of individual water communities (Figure 2b; Table S3). The remaining ASVs in each pool (6023 in sediments and 3145 in water) were absent in the other pool. Among the 547 ASVs, the percentage of abundant ASVs (relative abundance >0.1%) increased slightly, from 9% in the initial sediments (on day 0) and 8% in the sediments of the microcosms to 11% in the water fraction (Piecharts, Figure 2a). Rare ASVs (relative abundance <0.1%) comprised the majority of the overlapping ASVs for each fraction. These results suggested that a small fraction of the water communities, namely, ~15% in terms of ASV number was also detected in the sediment pool.

### 3.3 | Variability in taxonomic composition despite stable diversity along a POM quality gradient

At the end of the experiment, the realized species richness was, on average, higher in the microcosms containing high proportions of cyanobacteria (20D_80C and 100C) than in those in which diatoms predominated (80D_20C and 100D), but the difference was not significant (Figure 3a; ANOVA, $p > .1$). Evenness also did not significantly differ among any of the treatments (Figure 3b; Table S2). Conversely, β-diversity differed along POM quality gradients. POM addition had a significant effect on community composition in terms of taxonomic resemblance (PERMANOVA, pseudo-$F = 1.54$, $R^2 = .25$, $p = .04$) and phylogenetic, unweighted resemblance (pseudo-$F = 1.19$, $R^2 = .21$, $p = .02$) (Figure 3c,d, respectively), but not phylogenetic, weighted resemblance (Figure S5 and Table S4A). All three resemblances revealed similar overarching patterns (pairwise Mantel tests $p < .05$, Table S4B), suggesting that these patterns were robust.

The dominant bacterial classes were relatively stable along the gradient (Figure S6A). Members affiliated with *Campylobacteria* were overrepresented in all treatments, accounting for ~45% of

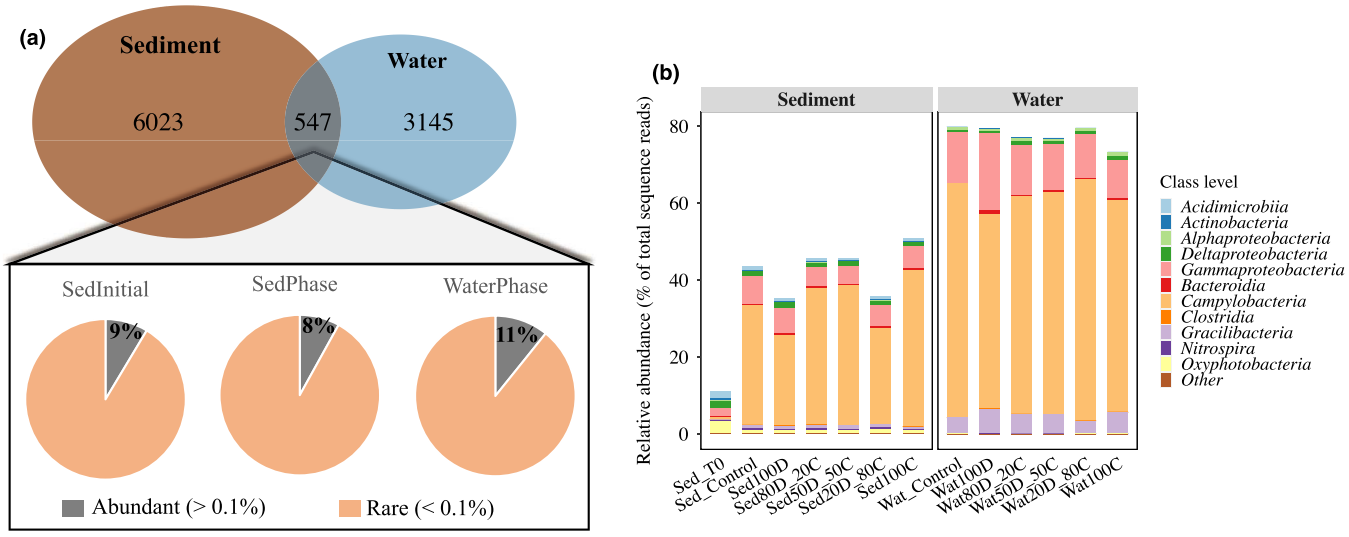


FIGURE 2 Venn diagram (a) illustrating the overlap of bacterial amplicon sequence variants (ASVs) found in the sediment and water samples, and pie-charts of the proportions of abundant and rare ASVs in the overlap. SedInitial, initial sediments (day 0); SedPhase, sediment phase of the microcosms on day 24; WaterPhase, water phase of the microcosms on day 24. The percentage in the pie-charts represents the number of abundant ASVs relative to the total number of shared ASVs. Abundant ASVs were defined as relative abundances >0.1%, and rare ASVs as relative abundances <0.1%, as described in Shen, Jürgens, et al. (2018). (b) Taxonomic affiliation of the shared ASVs at the class level. "Other" indicates the bacterial classes with a collective relative abundance of <0.1%

the individual communities, followed by *Gammaproteobacteria*, *Alphaproteobacteria*, Candidatus phylum radiation *Gracilibacteria* and *Bacteroidia*. The changes in the relative abundances of some orders or families along the POM gradients were consistent with those in the dominant classes, including *Acrobacteraceae*, *Bacteriovoracaceae*, *Flavobacteriaceae* and *JGI 0000069-P22* order, affiliated with the classes *Campylobacteria*, *Deltaproteobacteria*, *Bacteroidia* and *Gracilibacteria*, respectively (Figure S6B). However, not all orders or families affiliated with a particular class had identical responses. For instance, the relative abundances of *Caulobacteraceae* and *Rhodobacteraceae*, affiliated with *Alphaproteobacteria*, tended to be higher in treatments with a high cyanobacterial fraction whereas there was no clear trend for *SAR11_Clade III*. In the case of *Gammaproteobacteria*, the relative abundance along the POM gradient followed a pattern opposite that of *Nitrincolaceae*. Our results extended previous findings that many lineages within the *Caulobacteraceae* and *Rhodobacteraceae* are algae- and POM-associated, and favour cyanobacteria-originated POM, while the *SAR11* bacteria are usually free-living and adapted to oligotrophic environments (Dang & Lovell, 2016, and references therein).

## 3.4 | Identification of the phylogenetic relatedness of individual ASVs with shared POM preferences

A significant difference in the relative abundances between high diatom (100D and 80D_20C) and high cyanobacteria (100C and 20D_80C) additions was determined for 100 of the 3692 ASVs in the water samples (Figure 4; Table S5), representing about 20% of the individual communities (Figure 5b). Among the enriched ASV pool, ASV 16S_18 was the most abundant, with a maximum relative abundance of 2.79% in the 100D microcosms (Table S5). Clustering similar abundance patterns revealed two main clusters: one grouping the cyano-favoured taxa (72 ASVs) and the other the diatom-favoured taxa (28 ASVs) (Figure 4). The results of the ANOSIM showed that the two clusters differed significantly ($R$ = .51, $p$ = .001), despite variations in the relative abundance within each grouping. Although the responses of 100 ASVs determined were based on relative abundance, we also investigated the correlation between relative and absolute abundance for each of the 100 ASVs and found significant positive correlation between the two types of abundance data (Linear regression, lowest adjusted $R^2$ = .74 and $p$ < .001; Table S7). Generally, the overall community response measured in terms of relative abundances did not differ significantly from that in terms of absolute abundances (see Figure S7, Table S8 and Supporting Information text for details of the analyses using absolute abundance).

A phylogenetic tree was constructed to visualize the POM preferences and phylogenetic relatedness of the ASVs. The majority of the cyano-favoured ASVs were affiliated with *JGI 0000069-P22*, *Burkholderaceae*, *Rodobacteraceae* and *Nitrincolaceae* (Figure 5a, blue bar). The abundance of *JGI 0000069-P22* was eight-fold higher in the high cyanobacteria treatments than in the high diatom treatments (Figure 5a, outermost dashed line; Table S5). A similar but less pronounced response was observed for *Corynebacteriales*, *Ilumatobacteraceae*, *Crocinitomicaceae Hyphomonacaceae* and *Rhodocyclaceae*, the abundances of which increased ~six-fold.

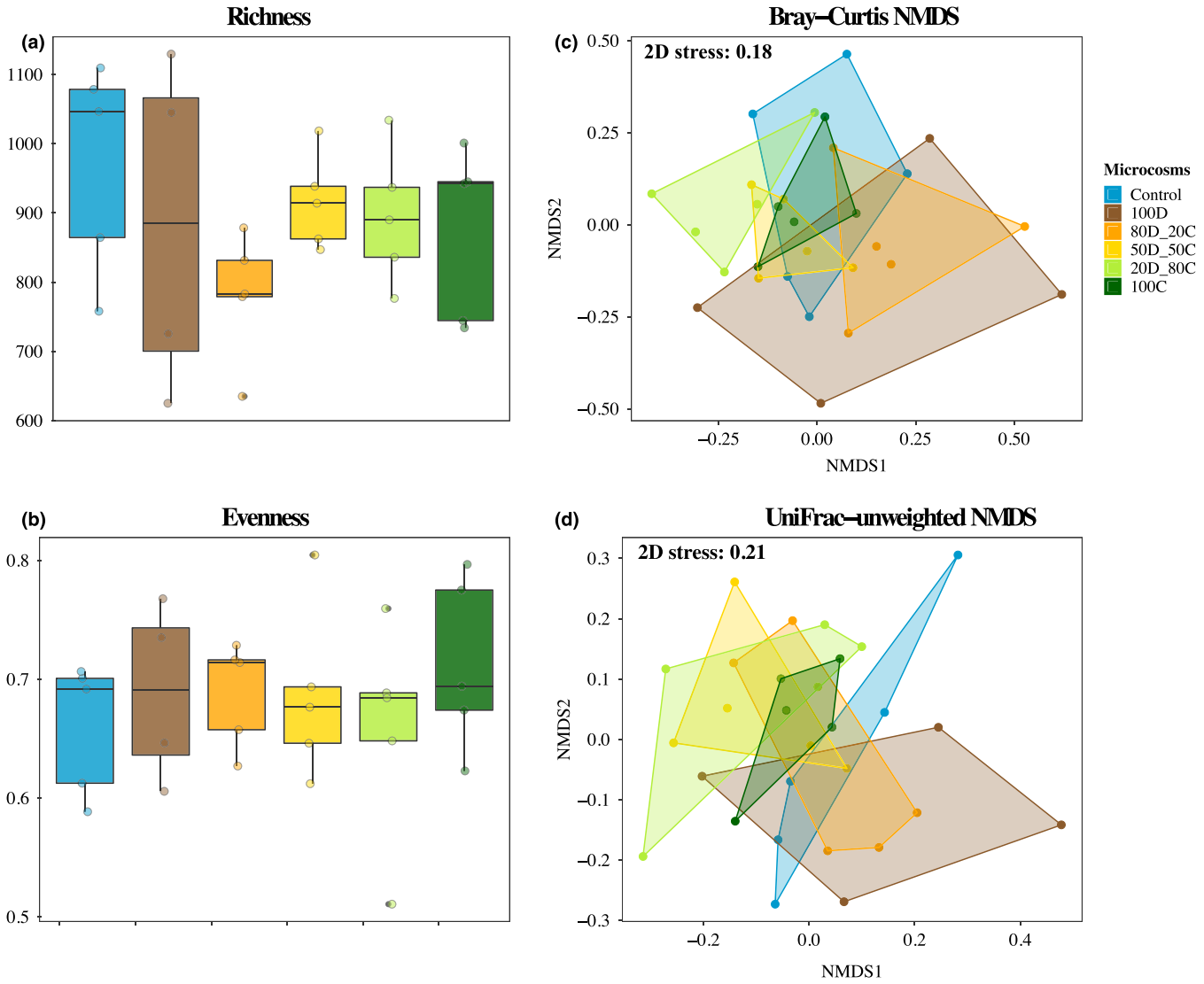


FIGURE 3 Within-sample (alpha) diversity (a, b) and between-sample (beta) diversity (c, d) of the bacterioplankton communities in microcosms with and without the addition of phytoplankton-originated particulate organic matter, after rarefaction to account for the sequencing effort among samples. (a) Observed species richness (total no. observed amplicon sequence variants), (b) evenness, (c) Bray–Curtis nonmetric multidimensional scaling (NMDS) (taxonomic, weighted resemblance), and (d) UniFrac-unweighted NMDS (phylogenetic, unweighted resemblance)

Diatom-favoured ASVs were mostly affiliated with *Methylophagaceae* and *Pseudomonadaceae*; their relative abundances increased ~six-fold compared to the high cyanobacteria treatments (Figure 5a, red bar; Table S5). Two ASVs affiliated with *Flavobacteriaceae* showed opposite preferences for phytoplankton-originated POM. Compared with other enriched bacterial families or orders, *Methylophagaceae* predominated in the control (9.34%) and in the 100D (14.02%), 80D_20C (8.92%), and 100C (3.41%) treatments (Figure 5b), and *Nitrincolaceae* in the 50D_50C (5.28%) and 20D_80C (4.89%) treatments (Figure 5b). These enriched bacterial taxa typically associate with organic matter degradation, as demonstrated in experimentally induced (Teeling et al., 2012) and natural (Buchan et al., 2014; Nowinski et al., 2019) phytoplankton blooms.

The phylogenetic relatedness analysis revealed that at the community level, ASVs with the two ecological categories were phylogenetically more closely related than random draws from a local pool of potential community members (diatom-favoured: NRI > +2, $p$ < .001; cyanofavoured: NRI > +2, $p$ < .002) (Table S6). Furthermore, the NTI analysis indicated that the observed phylogenetic clustering occurred at finer taxonomic scales, near the tips of the phylogenetic tree (diatom-favoured: NTI > +2, $p$ < .001; cyano-avoured: NTI > +2, $p$ < .001).

## 3.5 | Correlations between enriched taxa and inorganic nutrients

In addition to phylogenetic relatedness, we investigated potential correlations between any of the enriched taxa and inorganic nutrient concentrations (Table 1). An inverse relationship between the

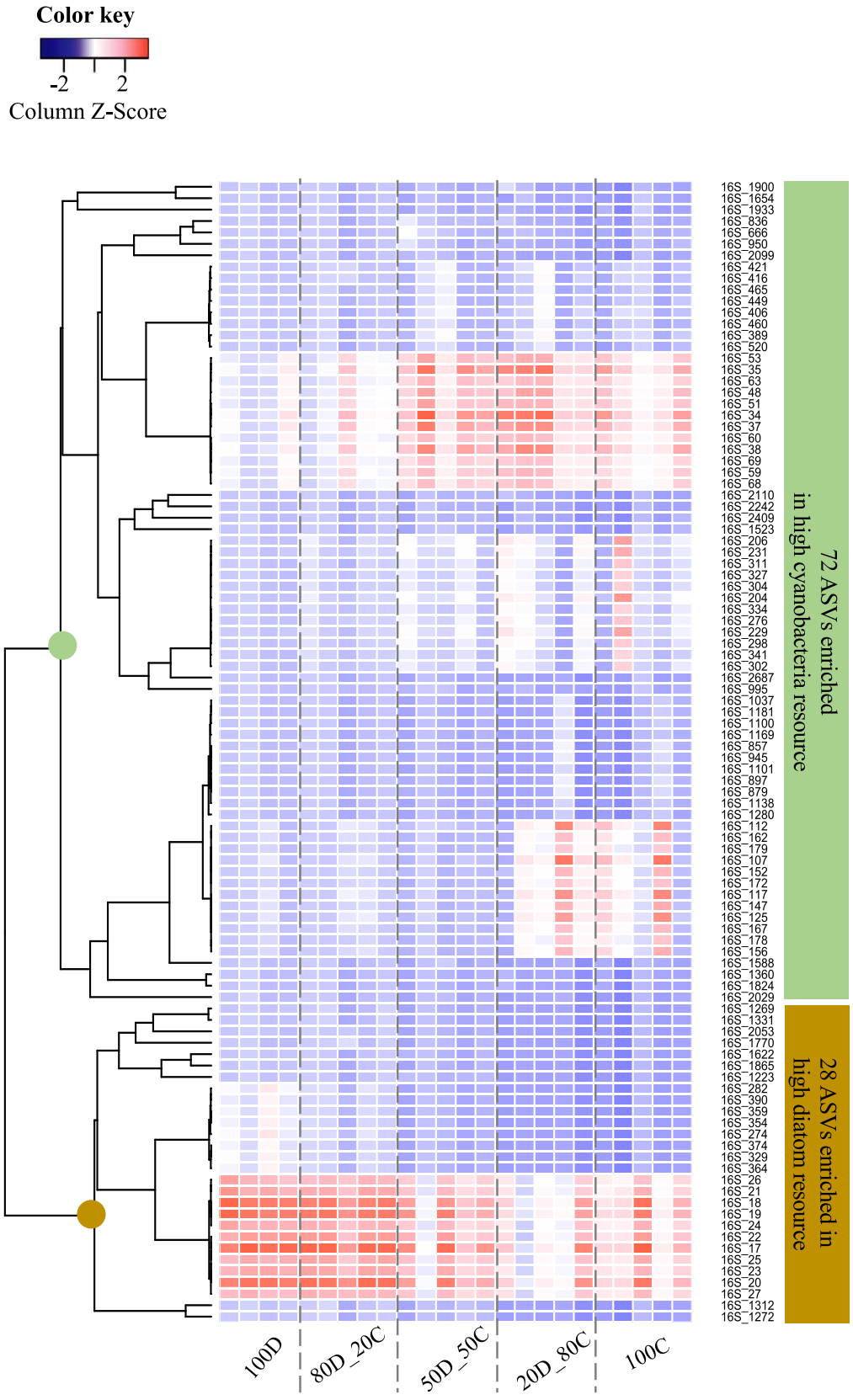


FIGURE 4 Heatmaps displaying the relative abundances of the enriched amplicon sequence variants (ASVs; 100 in total) across the POM quality gradient. Colour gradients represent the relative abundances of individual ASVs by column, with warm colours (towards red) indicating high abundances and cold colours (towards blue) low abundances within that sample. Column labels indicate the treatments (Figure 1), and row labels the ASVs. Dashed lines in the heatmaps separate the biological replicates according to the treatments. Side dendrograms cluster ASVs with similar occurrence patterns

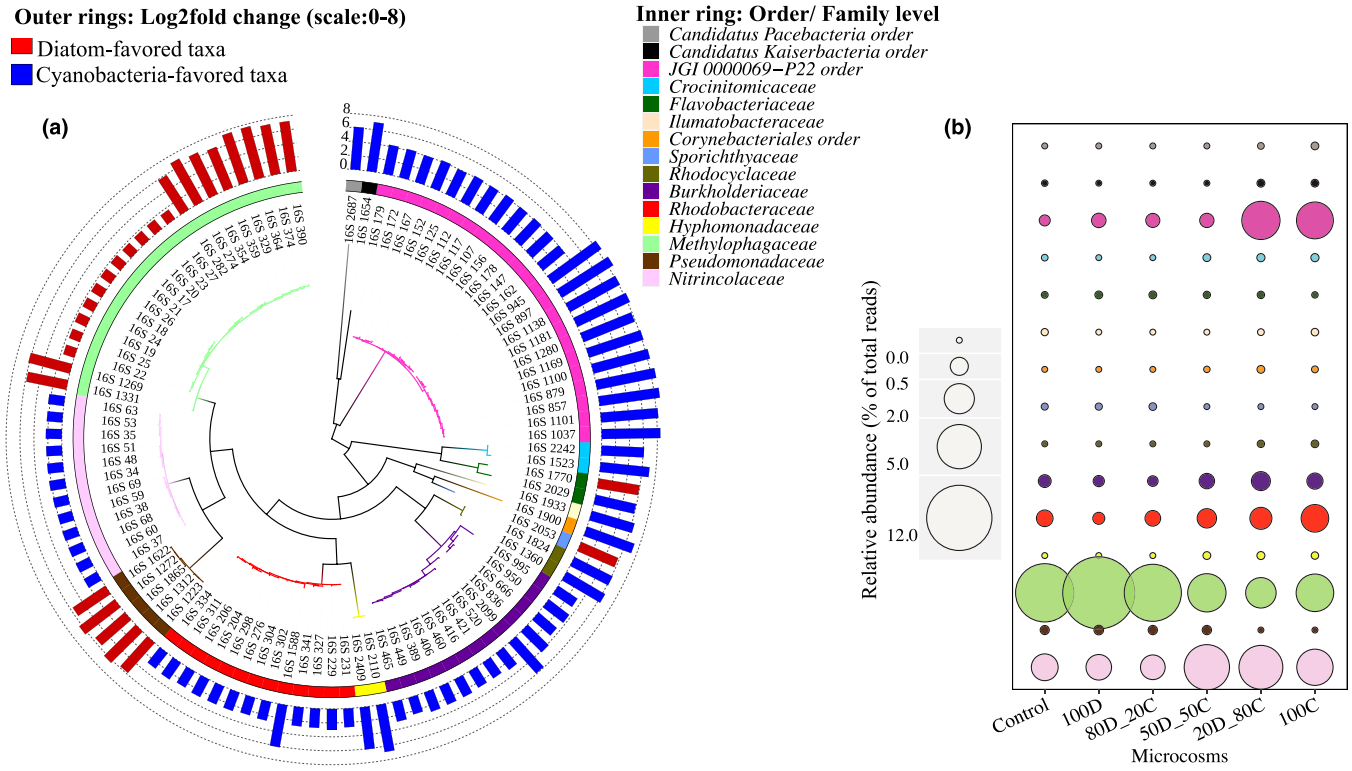


FIGURE 5 Phylogenetic relatedness and dynamics of bacterial ASVs whose relative abundances changed significantly along the POM quality gradient (high diatom vs. cyanobacteria addition). Only the ASVs that passed significant filtering are shown (see Table S5 for details on the differential abundance analysis). (a) Phylogenetic tree showing the phylogenetic distribution and enrichment of ASVs associated with phytoplankton-originated POM. Inner ring: taxonomic assignment of each ASV at the order and family levels. Outer-rings: each bar is colour-coded and indicates diatom-favoured or cyanobacteria-favoured taxa; the length of each bar indicates the fold change (log2) on a scale of 1–20 (dashed lines). (b) Bubble-plot illustrating taxon-specific dynamics in the controls and along the POM quality gradient. The size of the bubbles is proportional to the relative abundance calculated from the normalized reads, that is, the percentage of total sequence reads, and was determined based on the average value of biological replicates ($n$ = 5, but four replicates for the 100D treatments due to water loss during sampling)

relative abundances of most cyano-favoured taxa and the $NH_4^+$ concentration was determined and was statistically significant in three of the 12 correlations (Spearman's rho < 0, $p$ < .05). In the case of $PO_4^{3-}$ and NOx, the correlations with the relative abundances of these taxa were strongly positive (rho > 0; three significant cases and rho > 0; six significant cases, respectively, of 12 correlations). Conversely, diatom-favoured taxa tended to correlate positively with $NH_4^+$ (rho > 0; although not significant) but negatively with $PO_4^{3-}$ and NOx (rho < 0; 1 and 2 significant associations of four cases, respectively).

## 4 | DISCUSSION

The important roles of phytoplankton in connecting pelagic productivity to benthic ecosystems via POM export is well established (Franco et al., 2007; Griffiths et al., 2017). However, the assembly of bacterial communities at the water-sediment interface in response to heterogenous phytoplankton deposition is still poorly understood. In this study, we examined the response of the bacterial communities in the overlying water to POM inputs varying in their diatom- and cyanobacteria-derived proportions and the extent to which sediment bacteria contribute to that response. Our first hypothesis, that POM input alters bacterial communities, was supported with respect to β-diversity but not α-diversity, community turnover along the gradient was due to changes in the community membership rather than to differences in the total number of individuals. Previous studies (Finn et al., 2017; Landa et al., 2014; Nelson & Carlson, 2012) showed that bacterial diversity increased in the presence of available dissolved organic carbon derived from decaying phytoplankton. By contrast, in our study neither community richness nor evenness differed significantly among the treatments (Figure 3a,b). The stable α-diversity across the POM quality gradient may have reflected the initial bacterial diversity and/or the carrying capacity of a given community. The importance of initial diversity in understanding outcomes of community assembly has been pointed out (Roy et al., 2013; Shen, Langenheder, et al., 2018; Zha et al., 2016). The initial diversity of the community in the overlying water in the microcosms was likely to be low, as suggested by the total cell counts on day 7 of the experiment (Figure S4). Alternatively, the final water communities in

**TABLE 1** Spearman's correlation analyses showing the association between the relative abundance of the enriched taxa and the concentrations of ammonium ($NH_4^+$), phosphate ($PO_4^{3-}$) and integrated forms of nitrate and nitrite (NOx) across the microcosms

| | $NH_4^+$ | | $PO_4^{3-}$ | | NOx | |
|---|---|---|---|---|---|---|
| | Rho | *p*-Value | Rho | *p*-Value | Rho | *p*-Value |
| *Nitrincolaceae* | −.394 | .143 | .829 | **.021**** | .943 | **.002***** |
| *Hyphomonadaceae* | −.213 | .343 | .820 | **.023**** | .941 | **.003***** |
| *Rhodobacteraceae* | −.486 | .164 | .657 | .078 | .771 | **.036**** |
| *Burkholderiaceae* | −.371 | .234 | .771 | **.036**** | .943 | **.002**** |
| *Rhodocyclaceae* | −.845 | **.017**** | .304 | .279 | .541 | .134 |
| *Corynebacteriales order* | −.516 | .147 | .698 | .061 | .880 | **.010**** |
| *Illumatobacteraceae* | −.516 | .147 | .273 | .300 | .334 | .259 |
| *Flavobacteriaceae1* | −.845 | **.017**** | .304 | .279 | .541 | .134 |
| *Crocinitomicaceae* | −.464 | .177 | .638 | .087 | .812 | **.025**** |
| *JGI 0000069-P22 order* | −.657 | .078 | .257 | .311 | .600 | .104 |
| *Candidatus Kaiserbacteria order* | −.638 | .087 | .577 | .115 | .638 | .087 |
| *Candidatus Pacebacteria order* | −.845 | **.017**** | .304 | .279 | .541 | .134 |
| *Flavobacteriaceae2* | .029 | .521 | .086 | .436 | .429 | .198 |
| *Sporichthyaceae* | .152 | .387 | −.759 | **.040**** | −.941 | **.003***** |
| *Methylophagaceae* | .542 | .133 | −.714 | .055 | −.771 | **.036**** |
| *Pseudomonadaceae* | .696 | .062 | −.522 | .144 | −.493 | .160 |

Diatom-favoured taxa are denoted in red and cyanobacteria-favoured taxa in blue. *Flavobacteriaceae1* and *Flavobacteriaceae2* are two ASVs differing in their preference for phytoplankton-originated POM. A Spearman's Rho < 0 indicates a negative association, and a Rho > 0 a positive association. Significant *p*-values are indicated in bold: ***$p < .01$; **$p < .05$.

the microcosms may have been subjected to a carrying capacity that was similar along the POM gradient. Although total cell numbers increased substantially from day 7 to day 24 for all treatments, the differences in bacterial abundances were less pronounced among POM treatments than among the corresponding controls. It is therefore likely that the carrying capacity of the water column bacterial community was limited at the end of our experiment, thereby reducing potential contributions of "new taxa" (i.e., seedbank bacteria transiting from dormancy in the sediment to active growth) to community richness (Shade et al., 2014; Shen, Langenheder, et al., 2018).

Despite overlaps in community composition along the POM gradient, the variation in the beta diversity across treatments was significantly explained by the effects of diatom- or cyanobacteria-dominated resources (approximately 20%, Table S4A). This suggests that community dissimilarity is greater between-group than within-group. Our experiment was designed to examine how different POM mixtures (constant quantities but differing ratios of POM from a diatom and a cyanobacterium) affected the dynamics of the bacterial communities in the overlying water. Sarmento et al. (2016), in a study examining the importance of DOC quantity and quality in determining bacterial composition, found an inverse relationship between specialization and resource availability (quantity). In the presence of limited resource availability, few specialists are able to utilize specific types of organic matter effectively and thereby outperform generalists, whereas at increasing resource availability generalists readily exploit available resources regardless of their quality (Lennon et al., 2012; Sarmento et al., 2016). Overall, our findings indicate that the varying POM quality did not induce a community-level response toward resource specialization, at least not at a broad taxonomic level.

Although the relative abundances of the dominant bacterial classes were stable along the POM quality gradient, a higher proportion of bacterial ASVs was significantly enriched in the high cyanobacteria than in the high diatom treatments, which supported our second hypothesis (Figures 4 and 5). The addition of cyanobacteria- and diatom-originated POM in the microcosms may have selected for different sets of growth-promoting traits in bacteria associated with the two types of phytoplankton. OM released from diatoms includes complex and high molecular weight substrates (Luria et al., 2017), and the ability to utilize these substrates may be restricted to a few numbers of bacterial lineages. However, it has been suggested that less complex organic carbon molecules (e.g., glucose), are made available when cyanobacteria re-use and degrade extracellular organic carbon (Stuart et al., 2016). Those simple carbon can be readily assimilated by a great number of bacterial lineages. Furthermore, the observed phylogenetic clustering within either diatom- or cyanobacteria-favoured groups revealed that the distribution of those bacterial taxa more likely emerged by selection through filtering (Webb et al., 2002), such as their ability to utilize OM of varying molecular weight and composition (Thornton, 2014) above-discussed. Clustering at finer taxonomic scales, as indicated by high NTI further suggests the potential of functional redundancy among coexisting taxa, as closely related taxa tend to substantially

overlap in their functional repertoire (Martiny et al., 2015). In our study, *Methylophagaceae* were overrepresented among the significantly enriched taxonomic pool, with greater abundances in treatments containing higher amounts of diatom-originated POM, consistent with their preferential occurrence during/following diatom blooms (Landa et al., 2018). This group harbours the genus *Marine Methylotrophic Group 3* (Table S5), which belongs to the group of nonmethane-utilizing methylotrophs (Uhlig et al., 2018). Members of this group have been shown to utilize phytoplankton-derived C1 compounds such as methanol and methylamine (Bertrand et al., 2015).

We also found that cyano-favoured taxa tended to correlate with high $PO_4^{3-}$ and NOx concentrations, while the opposite was true for diatom-favoured taxa. $PO_4^{3-}$ accumulation over time in the microcosms most likely resulted from the OM degradation above and/or at the sediment surface, as shown to occur in the Baltic Sea (Schneider, 2011; van Helmond et al., 2020). The strong positive correlation between $PO_4^{3-}$ and NOx (Figure S3D) supports previous findings highlighting that phosphate availability can control the nitrification activity in marine sediment environments (Dang et al., 2013). The increase in NOx concentrations in the overlying water indicate that nitrification was an important process in our experimental sediments. Accordingly, changes in bacterial community composition in response to phytoplankton-originated POM input should impact the concentrations of inorganic nutrients involved in nitrification.

Our third hypothesis, that the response of bacterial assemblages in the overlying water could be a result of recruitment from actively growing sediment taxa, was not well-supported by our data. Specifically, there was little taxonomic overlap in the water and sediment communities of the microcosms (Figure 2a), which is in agreement with those of Walsh et al. (2016). Our results indicate that the formation of bacterial assemblages in the overlying water was unlikely to include recruitment from actively growing sediment taxa. Sediment resuspension occurring in natural systems involves not only the mixing of cells between sediments and overlying water, but also their respective environmental matrices. Presumably, in areas where sediment surface resuspension is high, the contribution of sediment microbes to the diversity and composition of the overlying water microbial assemblages can be larger than here estimated in our experiment. However, this did not rule out a potential role of sediment bacteria in modifying the microenvironment of the overlying water, such that particular taxa were favoured or disfavoured. The potential for priority effects on community assembly also cannot be excluded (Fukami, 2015). In marine environments, these often occur when the occupation of organic particles by early colonizers affects the establishment success of later colonizers (Dang & Lovell, 2016). Also, some bacteria tend to colonize particles faster than others (Dang et al., 2008; Datta et al., 2016), and thus impact or modify the interactions among bacteria in the surroundings. As such, the microorganisms that were the first to become established after POM addition, either from the sediment surface or the bottom water, may have influenced the community's ultimate response.

We acknowledge some limitations of our study. First, the selected diatom and cyanobacteria strains were cultured in the laboratory and did not account for the presence of other bloom-forming phytoplankton (e.g., dinoflagellates). Given the importance of bacteria-phytoplankton interactions, future work should consider a wider taxonomic representation of bloom-forming phytoplankton. Second, nano-sized cells and viruses able to pass through a 0.22 μm filter (Ghuneim et al., 2018) presumably coexisted with microbes originating from the water overlying the sediment in the microcosms. Consequently, our results should be interpreted as describing the potential dynamics of bacterial assemblages at the water-sediment interface. Nevertheless, even if our microcosms did not entirely replicate in situ conditions, our experimental data is useful for: (i) understanding the mechanisms that drive bacterial responses to phytoplankton-originated POM inputs, and (ii) evaluating potential interactions between bacteria and phytoplankton in the framework of benthic-pelagic coupling.

To conclude, we investigated the assembly and dynamics of bacterial communities at the water-sediment interface in relation to differences in the quality of phytoplankton-originated POM inputs. We found shifts in taxonomic composition across that gradient, and that sediment bacteria play minor roles in this process. Although not explored in this study, ecological interactions between heterotrophic microorganisms and phytoplankton play important roles in modulating carbon and nutrient cycles, not only in pelagic marine environments (Azam et al., 1994; Moran et al., 2016), but also in benthic ecosystems as indicated by our results. Given the sensitivity of phytoplankton to environmental disturbances, our study enables predictions on how the succession of different phytoplankton species may determine the coexistence and niche partitioning of heterotrophic bacteria inhabiting deep water. Future studies should extend the mechanistic understanding of community assembly and identify metabolic interactions among coexisting bacteria in the use of OM and metabolites derived from the deposited phytoplankton in sediments.

## ACKNOWLEDGEMENTS

This work was funded by the Swedish Research Council Formas (Grant no. 2016-00804 to FN and no. 2015-1320 to MW) and by the Swedish Environmental Protection Agency's Research Grant (NV-802-0151-18) to FN in collaboration with the Swedish Agency for Marine and Water Management. The authors wish to thank Per Hedberg and the staff at Askö laboratory for assistance in the field and during the experiment. We also acknowledge the support from the National Genomics Infrastructure in Stockholm funded by Science for Life Laboratory, the Knut and Alice Wallenberg Foundation and the Swedish Research Council, and SNIC/Uppsala Multidisciplinary Center for Advanced Computational Science for assistance with massively parallel sequencing and access to the UPPMAX computational infrastructure.

## CONFLICT OF INTEREST

The authors declare no competing interest.

## AUTHOR CONTRIBUTIONS

Dandan Izabel-Shen performed bioinformatics, analysed data, and wrote the paper with the help from Séréna Albert, Hanna Farnelid and Francisco J. A. Nascimento. Séréna Albert designed the experiment, conducted sampling and the experiment. Monika Winder contributed to the experimental design and commented on the manuscripts. Hanna Farnelid contributed to designing the experiment, performed DNA extraction and cell enumeration. Francisco J. A. Nascimento conceived and financed the study and designed the experiment. All authors discussed the results and commented on the manuscript.

## DATA AVAILABILITY STATEMENT

The FASTQ files and associated metadata have been made available in the European Nucleotide Archive under the accession number PRJEB39288. Our R scripts for statistics, data visualization and computing notes are available on Zenodo (https://doi.org/10.5281/zenodo.4743185) with supplement to GitHub (https://github.com/IzabelShen/PAPER_IzabelShen_AlgaPOM_2021).

## ORCID

*Dandan Izabel-Shen* https://orcid.org/0000-0002-3280-1166
*Séréna Albert* https://orcid.org/0000-0002-7299-7263
*Monika Winder* https://orcid.org/0000-0001-9467-3035
*Hanna Farnelid* https://orcid.org/0000-0003-3083-7437
*Francisco J. A. Nascimento* https://orcid.org/0000-0003-3722-1360

## REFERENCES

Amon, R. M. W., & Benner, R. (1996). Bacterial utilization of different size classes of dissolved organic matter. *Limnology and Oceanography*, *41*, 41–51. https://doi.org/10.4319/lo.1996.41.1.0041

Anderson, M. J. (2001). A new method for non-parametric multivariate analysis of variance. *Austral Ecology*, *26*, 32–46.

Azam, F., Smith, D. C., Steward, G. F., & Hagström, Å. (1994). Bacteria-organic matter coupling and its significance for oceanic carbon cycling. *Microbial Ecology*, *28*, 167–179.

Bertrand, E. M., McCrow, J. P., Moustafa, A., Zheng, H., McQuaid, J. B., Delmont, T. O., Post, A. F., Sipler, R. E., Spackeen, J. L., Xu, K., Bronk, D. A., Hutchins, D. A., & Allen, A. E. (2015). Phytoplankton–bacterial interactions mediate micronutrient colimitation at the coastal Antarctic sea ice edge. *Proceedings of the National Academy of Sciences of the United States of America*, *112*, 9938–9943.

Bray, J. R., & Curtis, J. T. (1957). An ordination of upland forest communities of southern Wisconsin. *Ecological Monographs*, *27*, 325–349.

Brown, M. R. (1991). The amino-acid and sugar composition of 16 species of microalgae used in mariculture. *Journal of Experimental Marine Biology and Ecology*, *145*, 79–99.

Buchan, A., LeCleir, G., Gulvik, C., & González, J. (2014). Master recyclers: Features and functions of bacteria associated with phytoplankton blooms. *Nature Reviews Microbiology*, *12*, 686–698.

Burd, A. B., & Jackson, G. A. (2009). Particle aggregation. *Annual Review of Marine Science 1*, 65–90.

Callahan, B. J., McMurdie, P. J., & Holmes, S. P. (2017). Exact sequence variants should replace operational taxonomic units in marker-gene data analysis. *ISME Journal*, *11*, 2639–2643.

Crump, B. C., Fine, L. M., Fortunato, C. S., Herfort, L., Needoba, J. A., Murdock, S., & Prahl, F. G. (2017). Quantity and quality of particular organic matter controls bacterial production in the Columbia River estuary. *Limnology and Oceanography*, *62*, 2713–2731.

Dang, H., Li, T., Chen, M., & Huang, G. (2008). Cross-ocean distribution of *Rhodobacterales* bacteria as primary surface colonizers in temperate coastal marine waters. *Applied and Environment Microbiology*, *74*, 52–60.

Dang, H., & Lovell, C. R. (2016). Microbial surface colonization and biofilm development in marine environments. *Microbiology and Molecular Biology Reviews*, *80*, 91–138.

Dang, H., Zhou, X., Yang, J., Ge, H., Jiao, N., Luan, X., Zhang, C., & Klotz, M. G. (2013). Thaumarchaeotal signature gene distribution in sediments of the northern South China Sea: An indicator of the metabolic intersection of the marine carbon, nitrogen, and phosphorus cycles? *Applied and Environment Microbiology*, *79*, 2137–2147.

Datta, M. S., Sliwerska, E., Gore, J., Polz, M. F., & Cordero, O. X. (2016). Microbial interactions lead to rapid micro-scale successions on model marine particles. *Nature Communications*, *7*, 11965.

Eiler, A., Langenheder, S., Bertillson, S., & Tranvik, L. J. (2003). Heterotrophic bacterial growth efficiency and community structure at different natural organic concentrations. *Applied and Environment Microbiology*, *69*, 3701–3709.

Farnelid, H., Turk-kubo, K., Ploug, H., Ossolinski, J. E., Collins, J. R., Van Mooy, B. A. S., & Zehr, J. P. (2019). Diverse diazotrophs are present on sinking particles in the North Pacific Subtropical Gyre. *ISME Journal*, *13*, 170–182.

Finn, D., Kopittke, P. M., Dennis, P. G., & Dalal, R. C. (2017). Microbial energy and matter transformation in agricultural soils. *Soil Biology & Biochemistry*, *111*, 176–192.

Franco, M. A., De Mesel, I., Demba Diallo, M., Van der Gucht, K., Van Gansbeke, D., van Rijswijk, P., Costa, M. J., Vincx, M., & Vanaverbeke, J. (2007). Effect of phytoplankton bloom deposition on benthic bacterial communities in two contrasting sediments in the southern North Sea. *Aquatic Microbial Ecology*, *48*, 241–254.

Fu, H., Uchimiya, M., Gore, J., & Moran, M. A. (2020). Ecological drivers of bacterial community assembly in synthetic phycospheres. *Proceedings of the National Academy of Sciences of the United States of America*, *117*, 3656–3662.

Fukami, T. (2015). Historical contingency in community assembly: Integrating niches, species pools, and priority effects. *Annual Review of Ecology and Systematics*, *46*, 1–23.

Gasol, J. M., & del Giorgio, P. A. (2000). Using flow cytometry for counting natural planktonic bacteria and understanding the structure of planktonic bacterial communities. *Scientia Marina*, *64*, 197–224.

Ghuneim, L. J., Jones, D. L., Golyshin, P. N., & Golyshina, O. V. (2018). Nano-sized and filterable bacteria and archaea: Biodiversity and function. *Frontiers in Microbiology*, *9*, 197.

Griffiths, J. R., Kadin, M. A., Nascimento, F. J. A., Tamelander, T., Törnroos, A., Bonaglia, S., Bonsdorff, E., Brüchert, V., Gårdmark, A., Järnström, M., Kotta, J., Lindegren, M., Nordström, M. C., Norkko, A., Olsson, J., Weigel, B., Žydelis, R., Blenckner, T., Niiranen, S., & Winder, M. (2017). The importance of benthic-pelagic coupling for marine ecosystem functioning in a changing world. *Global Change Biology*, *23*, 2179–2196.

Herlemann, D. P., Labrenz, M., Jürgens, K., Bertilsson, S., Waniek, J. J., & Andersson, A. F. (2011). Transitions in bacterial communities along the 2000 km salinity gradient of the Baltic Sea. *ISME Journal*, *5*, 1571–1579.

Hoikkala, L., Tammert, H., Lignell, R., Eronen-Rasimus, E., Spilling, K., & Kisand, V. (2016). Autochthonous dissolved organic matter drives bacterial composition during a bloom of filamentous cyanobacteria. *Frontiers in Marine Science*, *3*, 111.

Jones, S. E., & Lennon, J. T. (2010). Dormancy contributes to the maintenance of microbial diversity. *Proceedings of the National Academy of Sciences of the United States of America*, *107*, 5881–5886.

Karlsson, K., & Winder, M. (2018). Ecosystem effects of morphological and life history traits in two divergent zooplankton populations. *Frontiers in Marine Science*, *5*, 1–12.

Katoh, K., Misawa, K., Kuma, K., & Miyata, T. (2002). MAFFT: A novel method for rapid multiple sequence alignment based on fast Fourier transform. *Nucleic Acids Research*, *30*, 3059–3066.

Kembel, S. W., Cowan, P. D., Helmus, M. R., Cornwell, W. K., Morlon, H., Ackerly, D. D., Blomberg, S. P., & Webb, C. O. (2010). Picante: R tools for integrating phylogenies and ecology. *Bioinformatics*, *26*, 1463–1464.

Kirchman, D. L. (2003). The contribution of monomers and other low molecular weight compounds to the flux of DOM in aquatic ecosystems. In S. Findlay, & R. L. Sinsabaugh (Eds.), *Aquatic ecosystems-dissolved organic matter* (pp. 217–241). Academic Press.

Landa, M., Blain, S., Harmand, J., Monchy, S., Rapaport, A., & Obernosterer, I. (2018). Major changes in the composition of a Southern Ocean bacterial community in response to diatom-derived dissolved organic matter. *FEMS Microbiology Ecology*, *94*, fiy034.

Landa, M., Cottrell, M. T., Kirchman, D. L., Kaiser, K., Medeiros, P. M., Tremblay, L., Batailler, N., Caparros, J., Catala, P., Escoubeyrou, K., Oriol, L., Blain, S., & Obernosterer, I. (2014). Phylogenetic and structural response of heterotrophic bacteria to dissolved organic matter of different chemical composition in a continuous culture study. *Environmental Microbiology*, *16*, 1668–1681.

Larsson, U., Hajdu, S., Walve, J., & Elmgren, R. (2001). Baltic Sea nitrogen fixation estimated from the summer increase in upper mixed layer total nitrogen. *Limnology and Oceanography*, *46*, 811–820.

Lennon, J. T., Aanderude, Z. T., Lehmkuhl, B., & Schoolmaster, D. R. (2012). Mapping the niche space of soil microorganisms using taxonomy and traits. *Ecology*, *93*, 1867–1879.

Letunic, I., & Bork, P. (2019). InteractiveTree of Life (iTOL) v4: Recent updates and new developments. *Nucleic Acids Research*, *47*, W256–W259.

Lindh, M. V., Sjöstedt, J., Andersson, A. F., Baltar, F., Hugerth, L. W., Lundin, D., Muthusamy, S., Legrand, C., & Pinhassi, J. (2015). Disentangling seasonal bacterioplankton population dynamics by high-frequency sampling. *Environmental Microbiology*, *17*, 2459–2476.

Lozupone, C., & Knight, R. (2005). UniFrac: A new phylogenetic method for comparing microbial communities. *Applied and Environment Microbiology*, *71*, 8228–8235. https://doi.org/10.1128/AEM.71.12.8228-8235.2005

Luna, G. M., Manini, E., & Danovaro, R. (2002). Large fraction of dead and inactive bacteria in coastal marine sediments: Comparison of protocols for determination and ecological significance. *Applied and Environment Microbiology*, *68*, 3509–3519.

Luria, C. M., Amaral-Zettler, L. A., Ducklow, H. W., Pepeta, D. J., Rhyne, A. L., & Rich, J. J. (2017). Seasonal shifts in bacterial community response to phytoplankton-derived dissolved organic matter in the western Antarctic Peninsula. *Frontiers in Microbiology*, *8*, 2117.

Martiny, J. B. H., Jones, S. E., Lennon, J. T., & Martiny, A. C. (2015). Microbiomes in light of traits: A phylogenetic perspective. *Science*, *350*, 649–657.

Mestre, M., Ruiz-González, C., Logares, R., Duarte, C. M., Gasol, J. M., & Montserrat Sala, M. (2018). Sinking particles promote vertical connectivity in the ocean microbiome. *Proceedings of the National Academy of Sciences of the United States of America*, *115*, E6799–E6807.

Mitra, A., Skrzypczak, M., Ginalski, K., & Rowicka, M. (2015). Strategies for archiving high sequencing acurracy for low diversity samples and avoiding sample bleeding using Illumina plateform. *PLoS One*, *15*, e0227431.

Moran, M. A., Kujawinski, E. B., Stubbins, A., Fatland, R., Aluwihare, L. I., Buchan, A., Crump, B. C., et al. (2016). Deciphering ocean carbon in a changing world. *Proceedings of the National Academy of Sciences of the United States of America*, *113*, 3143–3151.

Mühlenbruch, M., Grossart, H., Eigemann, F., & Voss, M. (2018). Mini-review: Phytoplankton-derived polysaccharides in the marine environment and their interactions with heterotrophic bacteria. *Environmental Microbiology*, *20*, 2671–2685.

Nascimento, F. J. A., Karlson, A. M. L., & Elmgren, R. (2008). Settling blooms of filamentous cyanobacteria as food for meiofauna assemblages. *Limnology and Oceanography*, *53*, 2636–2643.

Nascimento, F. J. A., Karlson, A. M. L., Näslund, J., & Gorokhova, E. (2009). Settling cyanobacterial blooms do not improve growth condition for soft bottom meiofauna. *Journal of Experimental Marine Biology and Ecology*, *368*, 138–146.

Needham, D. M., & Fuhrman, J. A. (2016). Pronounced daily succession of phytoplankton, archaea and bacteria following a spring bloom. *Nature Microbiology*, *1*, 16005.

Nelson, C. E., & Carlson, C. A. (2012). Tracking differential incorporation of dissolved organic carbon types among diverse lineages of Sargasso Sea bacterioplankton. *Environmental Microbiology*, *14*, 1500–1516.

Nowinski, B., Smith, C. B., Thomas, C. M., Esson, K., Marin, R. 3rd, Preston, C. M., Birch, J. M., Scholin, C. A., Huntemann, M., Clum, A., Foster, B., Foster, B., Roux, S., Palaniappan, K., Varghese, N., Mukherjee, S., Reddy, T. B. K., Daum, C., Copeland, A., … Moran, M. A. (2019). Microbial metagenomes and metatranscriptomes during a coastal phytoplankton bloom. *Scientific Data*, *6*, 129.

Oksanen, A. J., Blanchet, F. G., Kindt, R., Minchin, P. R., Hara, R. B. O., Simpson, G. L., et al. (2011). *Vegan: Community ecology package*. https://cran.r-project.org/, https://github.com/vegandevs/vegan

Pinhassi, J., & Berman, T. (2003). Differential growth response of colony-forming alpha- and gamma-proteobacteria in dilution culture and nutrient addition experiments from Lake Kinneret (Israel), the eastern Mediterranean Sea, and the Gulf of Eilat. *Applied and Environment Microbiology*, *69*, 199–211.

Price, M. N., Dehal, P. S., & Arkin, A. P. (2009). FastTree: Computing large minimum evolution trees with profiles instead of a distance matrix. *Molecular Biology and Evolution*, *26*, 1641–1650.

Quast, C., Pruesse, E., Yilmaz, P., Gerken, J., Schweer, T., Yarza, P., Peplies, J., & Glöckner, F. O. (2013). The SILVA ribosomal RNA gene database project: Improved data processing and web-based tools. *Nucleic Acids Research*, *41*, D590–D596.

Reissmann, J. H., Burchard, H., Feistel, R., Hagen, E., Lass, H. U., Mohrholz, V., Nausch, G., Umlauf, L., & Wieczorek, G. (2009). Vertical mixing in the Baltic Sea and consequences for eutrophication – A review. *Progress in Oceanography*, *82*, 47–80.

Repeta, D. J., Quan, T. M., Aluwihare, L. I., & Accardi, A. (2002). Chemical characterization of high molecular weight dissolved organic matter in fresh and marine waters. *Geochimica et Cosmochimica Acta*, *66*, 955–962.

Romera-Castillo, C., Álvarez-Salgado, X. A., Galí, M., Gasol, J. M., & Marrasé, C. (2013). Combined effect of light exposure and microbial activity on distinct dissolved organic matter pools. A seasonal field study in an oligotrophic coastal system (Blanes Bay, NW Mediterranean). *Marine Chemistry*, *148*, 44–51.

Roy, K. D., Marzorati, M., Negroni, A., Thas, O., Balloi, A., Fabio, F., Verstraete, W., Daffonchio, D., & Boon, N. (2013). Environmental conditions and community evenness determine the outcome of biological invasion. *Nature Communications*, *4*, 1383.

Sarmento, H., Morana, C., & Gasol, J. M. (2016). Bacterioplankton niche partitioning in the use of phytoplankton-derived dissolved organic carbon: Quantity is more important than quality. *ISME Journal*, *10*, 2582–2592.

Schneider, B. (2011). PO4 release at the sediment surface under anoxic conditions: A contribution to the eutrophication of the Baltic Sea? *Oceanologia*, *53*, 415–429.

Shade, A., Jones, S. E., Caporaso, J. G., Handelsman, J., Knight, R., Fierer, N., & Gilbert, J. A. (2014). Conditionally rare taxa disproportionately

contribute to temporal changes in microbial diversity. *MBio*, *5*(4), e01371-14.

Shen, D., Jürgens, K., & Beier, S. (2018). Experimental insights into the importance of ecologically dissimilar bacteria to community assembly along a salinity gradient. *Environmental Microbiology*, *20*, 1170–1184. https://doi.org/10.1111/1462-2920.14059.

Shen, D., Langenheder, S., & Jürgens, K. (2018). Dispersal modifies the diversity and composition of active bacterial communities in response to a salinity disturbance. *Frontiers in Microbiology*, *9*, 2188. https://doi.org/10.3389/fmicb.2018.02188

Smith, H. J., Dieser, M., McKnight, D. M., SanClements, M. D., & Foreman, C. M. (2018). Relationship between dissolved organic matter quality and microbial community composition across polar glacial environments. *FEMS Microbiology Ecology*, *94*, fiy090.

Stegen, J. C., Lin, X., Konopka, A. E., & Fredrickson, J. K. (2012). Stochastic and deterministic assembly processes in subsurface microbial communities. *ISME Journal*, *6*, 1653–1664.

Stuart, R. K., Mayali, X., Lee, J. Z., Everroad, R. C., Hwang, M., Bebout, B. M., Weber, P. K., Pett-Ridge, J., & Thelen, M. P. (2016). Cyanobacterial reuse of extracellular organic carbon in microbial mats. *ISME Journal*, *10*, 1240–1251.

Taberlet, P., Bonin, A., Zinger, L., & Coissac, E. (2018). *Environmental DNA: For biodiversity research and monitoring*. Oxford University Press.

Teeling, H., Fuchs, B. M., Becher, D., Kkockow, C., Gardebrecht, A., Bennke, C. M., Kassabgy, M., Huang, S., Mann, A. J., Waldmann, J., Weber, M., Klindworth, A., Otto, A., Lange, J., Bernhardt, J., Reinsch, C., Hecker, M., Peplies, J., Bockelmann, F. D., … Amann, R. (2012). Substrate-controlled succession of marine bacterioplankton population induced by a phytoplankton bloom. *Science*, *336*, 608–611.

Thornton, D. C. O. (2014). Dissolved organic matter (DOM) release by phytoplankton in the contemporary and future ocean. *European Journal of Phycology*, *49*, 20–46.

Uhlig, C., Kirkpatrick, J. B., D'Hondt, S., & Loose, B. (2018). Methane-oxidizing seawater microbial communities from an Arctic shelf. *Biogeosciences*, *15*, 3311–3329.

Van Helmond, N. A. G. M., Robertson, E. K., Conley, D. J., Hermans, M., Humborg, C., Kubeneck, L. J., Lenstra, W. K., & Slomp, C. P. (2020). Removal of phosphorus and nitrogen in sediments of the eutrophic Stockholm archipelago, Baltic Sea. *Biogeosciences*, *17*, 2745–2766.

Walsh, E. A., Kirkpatrick, J. B., Rutherford, S. D., Smith, D. C., Sogin, M., & D'Hondt, S. (2016). Bacterial diversity and community composition from seasurface to subseafloor. *ISME Journal*, *10*, 979–989.

Wasmund, N., Tuimala, J., Suikkanen, S., Vandepitte, L., & Kraberg, A. (2011). Long-term trends in phytoplankton composition in the western and central Baltic Sea. *Journal of Marine Systems*, *87*, 145–159.

Webb, C. O., Ackerly, D. D., McPeek, M. A., & Donoghue, M. J. (2002). Phylogenies and community ecology. *Annual Review of Ecology and Systematics*, *33*, 475–505.

Wu, F. C., Tanoue, E., & Liu, C. Q. (2003). Fluorescence and amino acid characteristics of molecular size fractions of DOM in the waters of Lake Biwa. *Biogeochemistry*, *65*, 245–257.

Ye, L., Shi, X., Wu, X., Zhang, M., Yu, Y., Li, D., & Kong, F. (2011). Dynamics of dissolved organic carbon after a cyanobacterial bloom in hypereutrophic Lake Taihu (China). *Limnologica*, *41*, 382–388.

Zha, Y., Berga, M., Comte, J., & Langenheder, S. (2016). Effects of dispersal and initial diversity on the composition and functional performance of bacterial communities. *PLoS One*, *11*, e0155239.

Zinger, L., Amaral-Zettler, L. A., Fuhrman, J. A., Horner-Devine, M. C., Huse, S. M., Welch, D. B. M., Martiny, J. B. H., Sogin, M., Boetius, A., & Ramette, A. (2011). Global patterns of bacterial beta-diversity in seafloor and seawater ecosystems. *PLoS One*, *6*, e24570.

Zinger, L., Bonin, A., Alsos, I. G., Bálint, M., Bik, H., Boyer, F., Chariton, A. A., Creer, S., Coissac, E., Deagle, B. E., De Barba, M., Dickie, I. A., Dumbrell, A. J., Ficetola, G. F., Fierer, N., Fumagalli, L., Gilbert, M. T. P., Jarman, S., Jumpponen, A., … Taberlet, P. (2019). DNA metabarcoding – Need for robust experimental designs to draw sound ecological conclusions. *Molecular Ecology*, *28*, 1857–1862.

## SUPPORTING INFORMATION

Additional supporting information may be found online in the Supporting Information section.

**How to cite this article:** Izabel-Shen, D., Albert, S., Winder, M., Farnelid, H., & Nascimento, F. J. A. (2021). Quality of phytoplankton deposition structures bacterial communities at the water-sediment interface. *Molecular Ecology*, 30, 3515–3529. https://doi.org/10.1111/mec.15984

*Supplemental information for*

# Quality of phytoplankton deposition structures bacterial communities at the water-sediment interface

Dandan Izabel-Shen[1#*], Séréna Albert[1#], Monika Winder[1], Hanna Farnelid[2], Francisco J. A. Nascimento[1]

*1 Department of Ecology, Environment and Plant Sciences, Stockholm University, Stockholm, Sweden*

*2 Center for Ecology and Evolution in Microbial Model Systems, Linnaeus University, Kalmar, Sweden*

#The authors contributed equally to this work.

*Correspondence:

Dandan Izabel-Shen, dand.shen@gmail.com, Department of Ecology, Environment and Plant Sciences, Stockholm University, Stockholm, Sweden.

Contents:

**Supplementary Figure S1** Example of cytogram from seawater sample "167B" stained with SYBR showing green fluorescence (FL1) versus granularity (SSC) and the applied gate for counting bacteria cells (red).

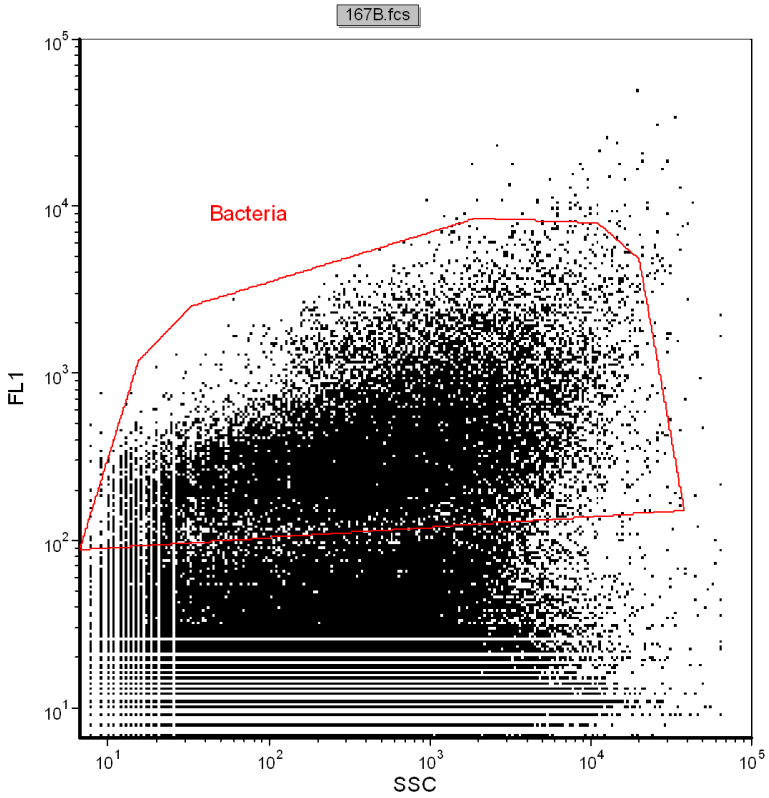

**Supplementary Figure S2** Taxonomic composition of bacterial associates in the phytoplankton slurries. '*Skeleton*' refers to slurries of the diatom *Skeletonema marinoi*, and '*Nodularia*' to the slurries of the cyanobacterium *Nodularia spumigena*. The terminal number represents the technical replicate. The first panel displays the relative abundance of dominant bacterial classes associated to the phytoplankton slurries. The other panels present the bacterial families affiliated with each of the dominant classes.

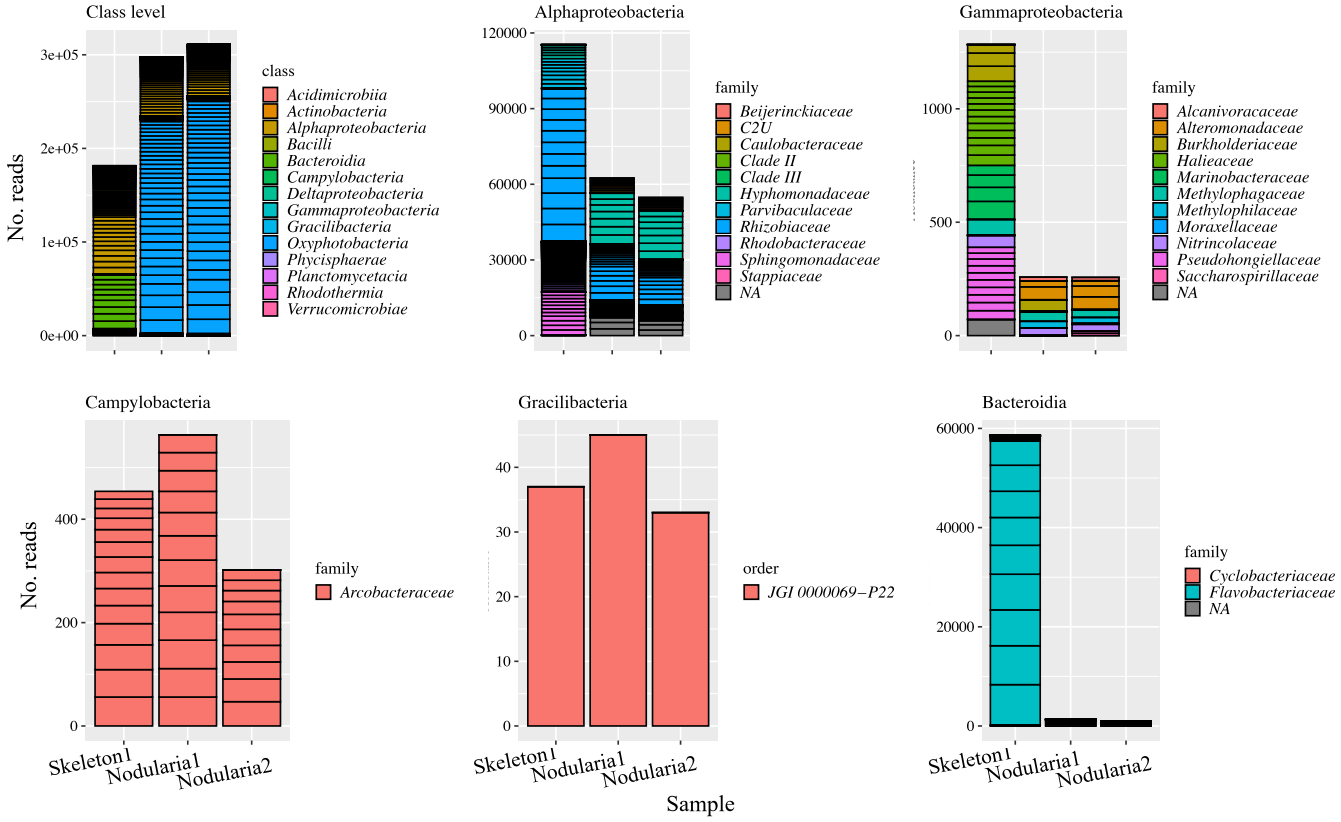

**Supplementary Figure S3** The concentrations of $NH_4^-$ **A)**, $PO_4^{3-}$ **B**) and NOx **C**) at the beginning (T0) and end (Tf) of the experiment and their correlations at Tf **D**). A one-way repeated measurement ANOVA was used to test the effect of POM addition, time and their interaction on the concentrations of inorganic nutrients. A one-way ANOVA was further used to test the effect of POM addition on NOx concentrations across microcosms for each time point. The significance levels are shown in the figure: *** $P < 0.001$ ** $P < 0.01$ * $P < 0.05$. a–c indicate significant post-hoc groups ($P$-adj <0.1) determined in Tukey post-hoc tests corrected for multiple comparisons. Bold and non-bold letters on panel C indicate post-hoc groups from different time points.

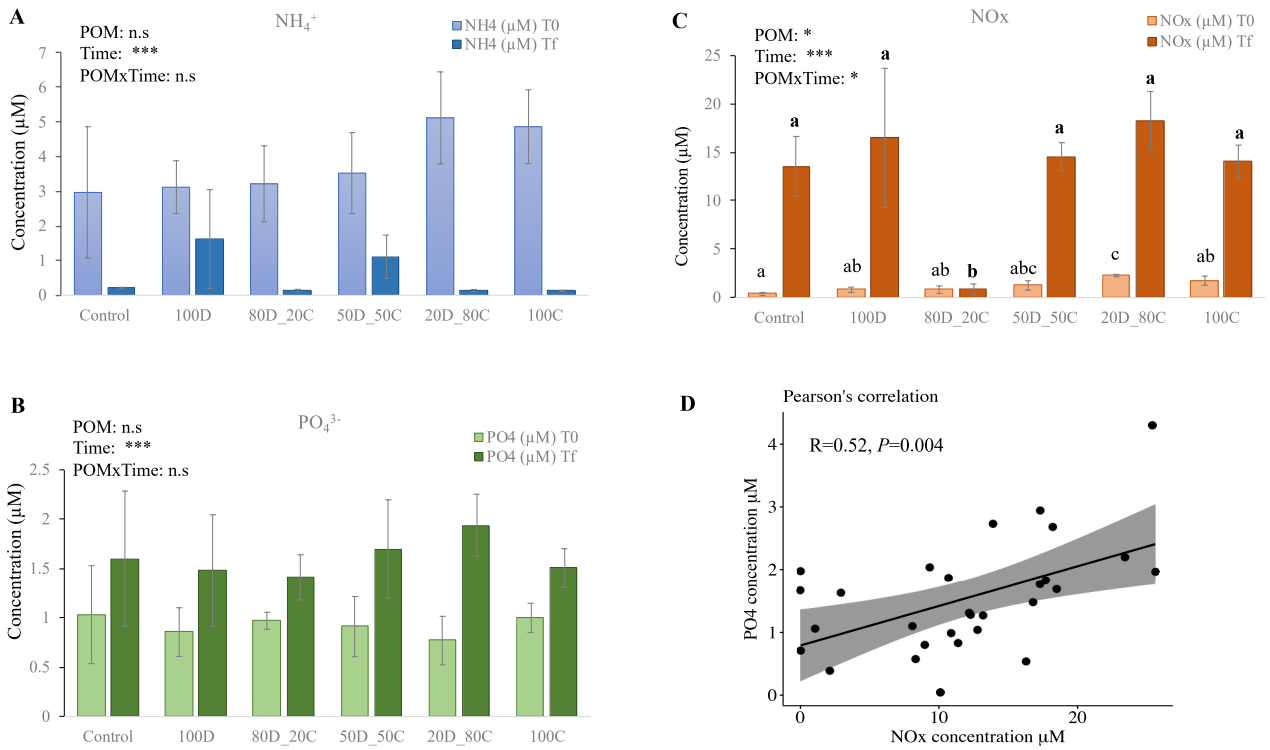

**Supplementary Figure S4** Total bacterial cell abundances on day 7 and day 24 measured using flow cytometry. Repeated-measurement ANOVA tests with replicates as the randomized blocking factor show significant effects of POM addition ($P$ <0.001), time ($P$ <0.001) and POM addition × time ($P$ <0.001) on the total bacterial abundances over time and across microcosms. A one-way ANOVA was used to test the effect of POM addition on bacterial abundances on day 7 and day 24. The letters a and b indicate significant post-hoc groups ($P$-adj <0.1) determined in Tukey post-hoc tests with correction for multiple comparisons.

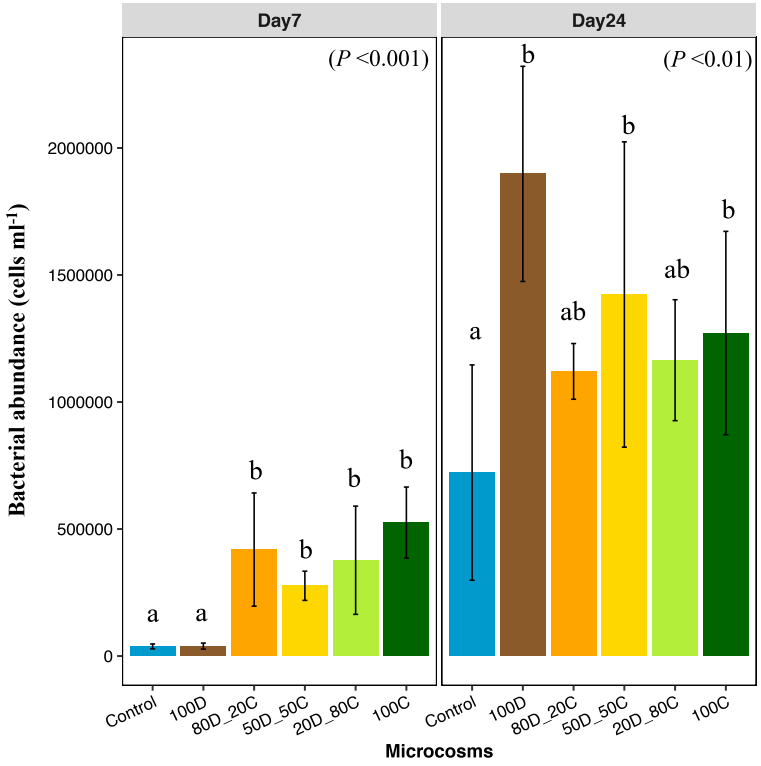

**Supplementary Figure S5** Between-sample(beta) diversity calculated with the weighted UniFrac dissimilarity and visualized in a non-multidimensional scaling plot. 2D stress value: 0.11.

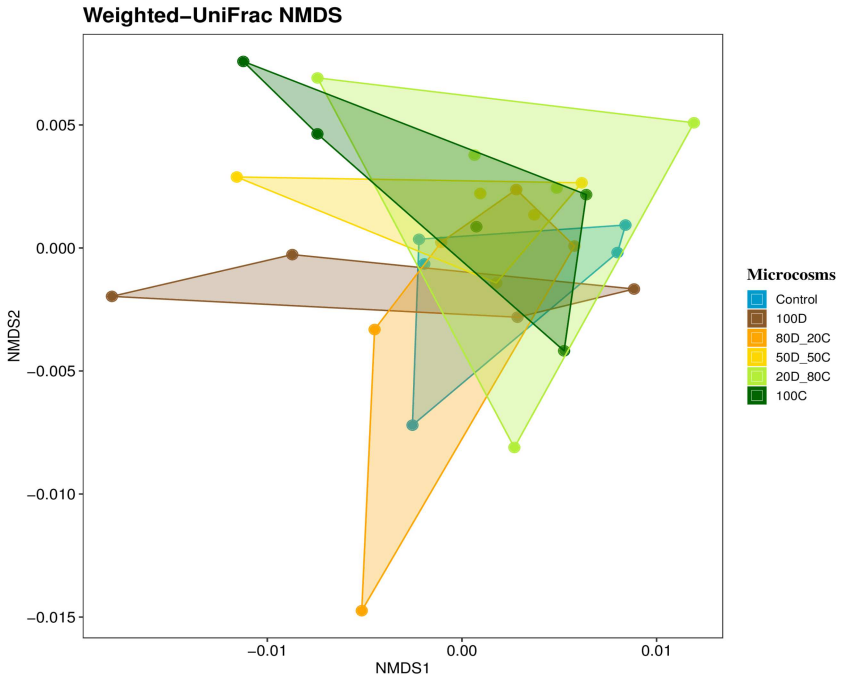

**Supplementary Figure S6** Compositional responses to POM resource addition at the class **A)** and family **B)** levels. Other: all ASVs assigned to bacterial classes with a collective relative abundance of <1%.

**A**

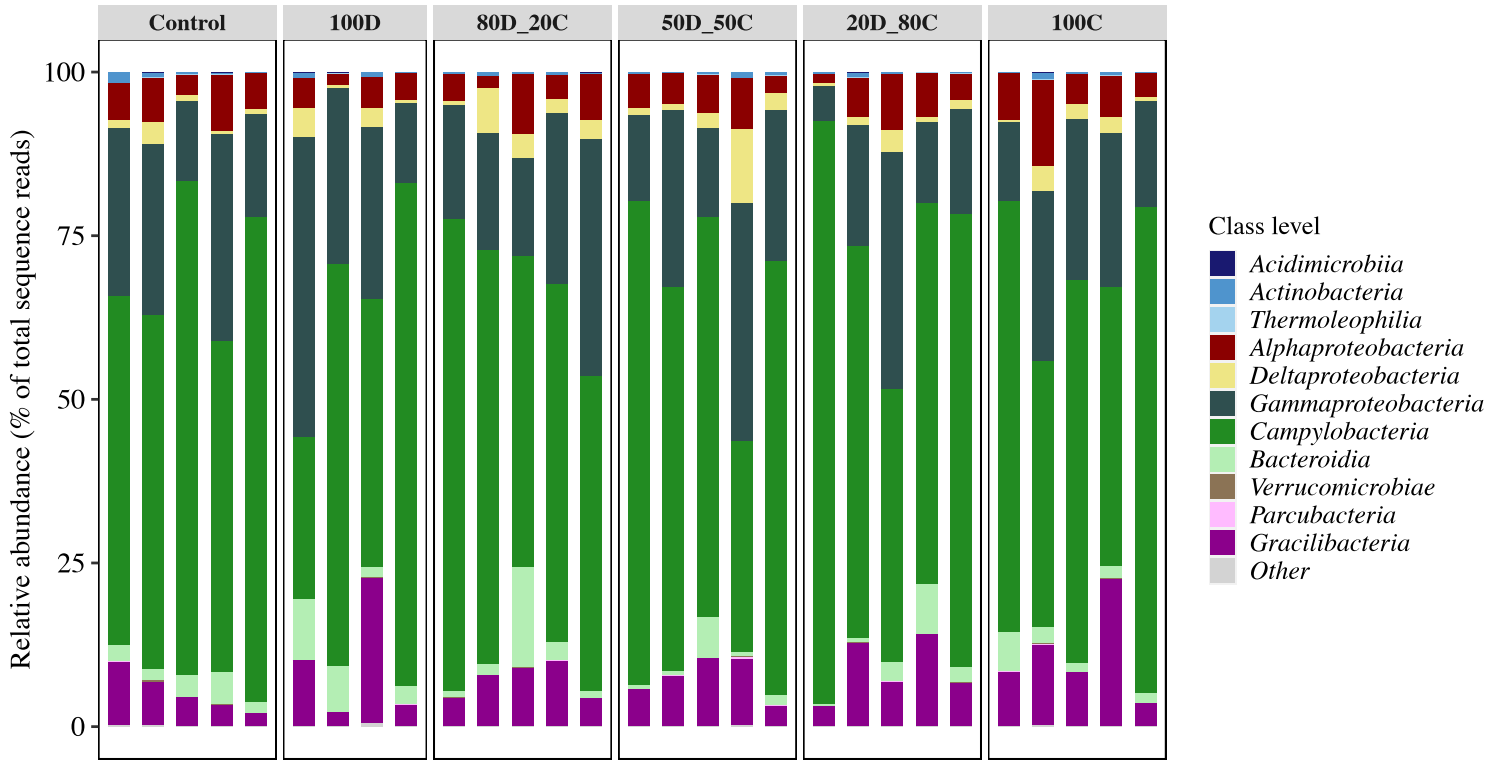

**B**

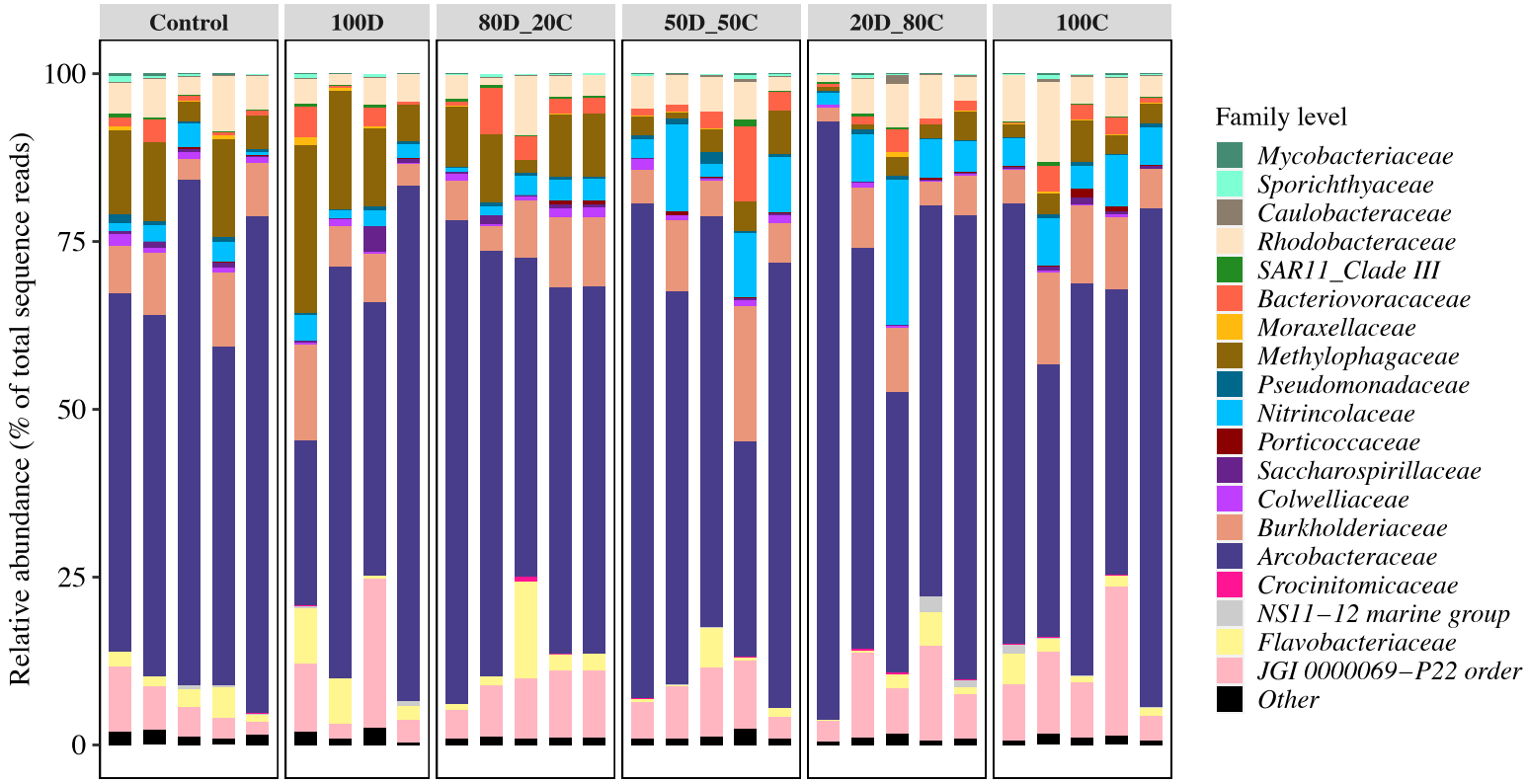
Control
100D
80D_20C
50D_50C
20D_80C
100C
Relative abundance (% of total sequence reads)
100
75
50
25
0
Family level
Mycobacteriaceae
Sporichthyaceae
Caulobacteraceae
Rhodobacteraceae
SAR11_Clade III
Bacteriovoracaceae
Moraxellaceae
Methylophagaceae
Pseudomonadaceae
Nitrincolaceae
Porticoccaceae
Saccharospirillaceae
Colwelliaceae
Burkholderiaceae
Arcobacteraceae
Crocinitomicaceae
NS11−12 marine group
Flavobacteriaceae
JGI 0000069−P22 order
Other

**Supplementary Table S1** Inorganic nutrient content and bacterial abundances in each biological replicate in the microcosms. POM resource gradients differing in their diatom (D) and cyanobacteria (C) contributions (%) were established as follows: 100D; 80D_20C, 50D_50C; 20D_80C, 100C. Control microcosms contained no added POM. The terminal number represents the biological replicate. NA: no available data; D0: day 0 (start of the experiment), D7: day 7, D24: day 24 (end of the experiment).

| Sample ID | NH4-N_D0 (µM) | PO4-P_D0 (µM) | NOx_D0 (µM) | NH4-N_D24 (µM) | PO4-P_D24 (µM) | Nox_D24 (µM) | Bacteria_ D7 (cell $ml^{-1}$) | Bacteria_D24 (cell $ml^{-1}$) |
|---|---|---|---|---|---|---|---|---|
| Control 1 | 1.18 | 0.48 | 0.24 | 0.23 | 1.04 | 12.80 | 2.60E+04 | 3.63E+05 |
| Control 2 | 0.225 | 0.07 | 0.05 | 0.18 | 0.80 | 9.00 | 3.52E+04 | 3.47E+05 |
| Control 3 | 3 | 1.21 | 0.77 | 0.24 | 1.28 | 12.30 | 3.87E+04 | 7.39E+05 |
| Control 4 | 10.3 | 2.88 | 0.74 | 0.25 | 4.30 | 25.40 | 3.68E+04 | 7.72E+05 |
| Control 5 | 0.16 | 0.51 | 0.03 | 0.15 | 0.58 | 8.34 | 5.30E+04 | 1.39E+06 |
| 100D 1 | 2.11 | 0.06 | 0.21 | 0.29 | 0.54 | 16.30 | 2.90E+04 | 1.31E+06 |
| 100D 2 | 5 | 0.98 | 1.19 | 0.22 | 2.04 | 9.35 | 4.00E+04 | 1.73E+06 |
| 100D 3 | 3.17 | 0.90 | 1.43 | 0.10 | 0.99 | 10.90 | 2.53E+04 | 1.84E+06 |
| 100D 4 | 0.84 | 0.74 | 0.09 | 0.14 | 0.39 | 2.16 | 4.95E+04 | 2.24E+06 |
| 100D 5 | 4.51 | 1.60 | 1.11 | 0.139 | 0.392 | 2.16 | 5.21E+04 | 2.37E+06 |
| 80D_20C 1 | 0.222 | 0.77 | 0.07 | 0.27 | 1.63 | 2.96 | 1.56E+05 | 1.07E+06 |
| 80D_20C 2 | 1.17 | 0.78 | 0.33 | 0.13 | 0.71 | 0.06 | 7.09E+05 | 1.25E+06 |
| 80D_20C 3 | 3.8 | 1.10 | 0.31 | 0.11 | 1.67 | 0.03 | 5.79E+05 | 1.18E+06 |
| 80D_20C 4 | 6.05 | 1.01 | 2.17 | 0.10 | 1.06 | 1.10 | 3.61E+05 | 1.14E+06 |

| Sample ID | NH4-N_D0 (µM) | PO4-P_D0 (µM) | NOx_D0 (µM) | NH4-N_D24 (µM) | PO4-P_D24 (µM) | NOx_D24 (µM) | Bacteria_ D7 (cell $ml^{-1}$) | Bacteria_D24 (cell $ml^{-1}$) |
|---|---|---|---|---|---|---|---|---|
| 80D_20C 5 | 4.87 | 1.20 | 1.21 | 0.08 | 1.98 | 0.05 | 2.91E+05 | 9.63E+05 |
| 50D_50C 1 | 4.78 | 1.71 | 2.30 | 2.30 | 2.73 | 13.90 | 3.68E+05 | 1.01E+06 |
| 50D_50C 2 | 6.8 | 1.34 | 1.80 | 2.95 | 1.77 | 17.30 | 2.66E+05 | 9.26E+05 |
| 50D_50C 3 | 1.24 | 0.05 | 0.11 | 0.10 | 0.04 | 10.10 | 2.91E+05 | 1.03E+06 |
| 50D_50C 4 | 0.488 | 1.07 | 0.03 | 0.13 | 2.68 | 18.20 | 2.28E+05 | 1.97E+06 |
| 50D_50C 5 | 4.36 | 0.39 | 2.02 | 0.08 | 1.27 | 13.20 | 2.30E+05 | 2.18E+06 |
| 20D_80C 1 | 8.11 | 1.60 | 2.43 | 0.26 | 2.94 | 17.30 | 3.16E+05 | 1.06E+06 |
| 20D_80C 2 | 2.65 | 0.46 | 2.10 | 0.12 | 1.10 | 8.11 | 1.78E+05 | 1.18E+06 |
| 20D_80C 3 | 1.45 | 0.15 | 1.99 | 0.10 | 1.48 | 16.80 | 1.89E+05 | 1.03E+06 |
| 20D_80C 4 | 5.75 | 0.96 | 2.71 | 0.11 | 1.97 | 25.60 | 6.34E+05 | 9.83E+05 |
| 20D_80C 5 | 7.69 | 0.68 | 2.15 | 0.09 | 2.20 | 23.40 | 5.69E+05 | 1.57E+06 |
| 100C 1 | 2.91 | 0.71 | 1.07 | 0.20 | 1.31 | 12.20 | 5.20E+05 | 1.46E+06 |
| 100C 2 | 8.68 | 1.39 | 2.27 | 0.13 | 1.87 | 10.70 | 3.98E+05 | 8.78E+05 |
| 100C 3 | 2.91 | 0.65 | 0.22 | 0.08 | 0.83 | 11.40 | 5.28E+05 | 8.09E+05 |
| 100C 4 | 4.34 | 0.96 | 2.74 | 0.10 | 1.69 | 18.50 | 4.27E+05 | 1.52E+06 |
| 100C 5 | 5.53 | 1.29 | 2.46 | 0.11 | 1.83 | 17.70 | 7.54E+05 | 1.69E+06 |

**Supplementary Table S2** Number of sequence reads retrieved from sediment and water samples, the percentage of sequence reads of phytoplankton slurries-derived ASVs relative to the total reads of the sediment and water samples, and bacterial community diversity metrics in the water column of the microcosms. POM resource gradients differing in their diatom (D) and cyanobacteria (C) contributions (%) were established as follows: 100D; 80D_20C, 50D_50C; 20D_80C, 100C. Control microcosms contained no added POM. NA, no available data; Sed_D0, initial sediment samples on day 0 (beginning of the experiment); 'sediment' and "water" indicate the origin of samples; Uniq_Slu%: the number of sequence reads of the ASVs present only in the phytoplankton slurries not in the control microcosms of the water phase or in the initial sediment samples or control microcosms of the sediments. Those 'Uniq_Slu' ASVs were filtered out from the total reads of sediment and water samples prior to subsampling.

| Sampl ID | Uniq_Slu% (sediment) | No.reads (sediment) | Uniq_Slu% (water) | No.reads (water) | Richness (water) | Evenness (water) |
|---|---|---|---|---|---|---|
| *Skeleton.*_Slu | 0.997 | NA | 0.966 | NA | NA | NA |
| *Nodularia*_Slu 1 | 0.991 | NA | 0.985 | NA | NA | NA |
| *Nodularia*_Slu 2 | 0.992 | NA | 0.986 | NA | NA | NA |
| Sed_D0 1 | 0 | 17,476 | NA | NA | NA | NA |
| Sed_D0 2 | 0 | 24,972 | NA | NA | NA | NA |
| Sed_D0 3 | 0 | 29,089 | NA | NA | NA | NA |
| Sed_D0 4 | 0 | 15,768 | NA | NA | NA | NA |
| Sed_D0 5 | 0 | 24,777 | NA | NA | NA | NA |
| Control 1 | 0 | 24,199 | 0 | 310,278 | 1078.50 | 0.69 |
| Control 2 | 0 | 13,517 | 0 | 319,835 | 1109.50 | 0.70 |
| Control 3 | 0 | 27,341 | 0 | 577,885 | 1046.50 | 0.59 |
| Control 4 | 0 | 27,929 | 0 | 342,893 | 864.50 | 0.71 |
| Control 5 | 0 | 22,503 | 0 | 494,454 | 758.00 | 0.61 |

| Sampl ID | Uniq_Slu (sediment) | No.reads (sediment) | Uniq_Slu% (water) | No.reads (water) | Richness (water) | Evenness (water) |
|---|---|---|---|---|---|---|
| 100D 1 | 0.002 | 21,243 | 0.0009 | 301,979 | 1129.50 | 0.77 |
| 100D 2 | 0 | 22,166 | 0.0006 | 326,512 | 725.50 | 0.65 |
| 100D 3 | 0.002 | 27,927 | 0.0003 | 348,142 | 1045.00 | 0.74 |
| 100D 4 | 0 | 33,350 | 0.0001 | 338,621 | 625.00 | 0.61 |
| 100D 5 | 0 | 26,675 | NA | NA | NA | NA |
| 80D_20C 1 | 0 | 29,344 | 0.0004 | 354,708 | 635.00 | 0.63 |
| 80D_20C 2 | 0 | 17,247 | 0 | 369,355 | 831.50 | 0.66 |
| 80D_20C 3 | 0.003 | 21,471 | 0.0002 | 331,313 | 779.00 | 0.73 |
| 80D_20C 4 | 0.001 | 25,334 | 0.0001 | 260,467 | 783.00 | 0.71 |
| 80D_20C 5 | 0.004 | 23,063 | 0.0002 | 276,567 | 878.50 | 0.72 |
| 50D_50C 1 | 0 | 31,452 | 0 | 448,852 | 914.00 | 0.61 |
| 50D_50C 2 | 0.003 | 31,269 | 0.0002 | 273,068 | 847.00 | 0.69 |
| 50D_50C 3 | 0.005 | 22,086 | 0.0007 | 391,319 | 1018.50 | 0.68 |
| 50D_50C 4 | 0.004 | 30,743 | 0.0020 | 193,380 | 938.50 | 0.80 |
| 50D_50C 5 | 0.003 | 26,108 | 0.0002 | 313,384 | 862.50 | 0.65 |
| 20D_80C 1 | 0 | 31,722 | 0.0001 | 736,852 | 836.00 | 0.51 |
| 20D_80C 2 | 0.008 | 43,985 | 0.0014 | 303,868 | 890.00 | 0.69 |
| 20D_80C 3 | 0.031 | 41,743 | 0.0001 | 270,253 | 1034.00 | 0.76 |
| 20D_80C 4 | 0 | 45,047 | 0.0003 | 346,663 | 776.50 | 0.68 |
| 20D_80C 5 | 0.003 | 59,777 | 0.0004 | 311,680 | 937.00 | 0.65 |
| 100C 1 | 0.002 | 25,784 | 0.0002 | 289,148 | 744.50 | 0.67 |
| 100C 2 | 0.012 | 26,266 | 0.0007 | 187,434 | 942.50 | 0.80 |
| 100C 3 | 0.003 | 31,686 | 0.0012 | 298,298 | 1001.00 | 0.69 |
| 100C 4 | 0.004 | 19,665 | 0.0020 | 241,102 | 945.00 | 0.78 |
| 100C 5 | 0.006 | 34,373 | 0.0005 | 240,318 | 734.00 | 0.62 |

**Supplementary Table S4** The results of permutational multivariate analysis of variance (PERMANOVA) testing the effect of phytoplankton-originated POM on bacterioplankton community composition **A**), and Mantel test for pairwise comparison between two of dissimilarity matrices **B**). $R^2$ in the PERMANOVA indicates the variance explaining community variation.

**A)**

| | Pesudo-F | $R^2$ | P-value |
|---|---|---|---|
| Bray-Curtis dissimilarity | 1.5439 | 0.251 | 0.044* |
| Weighted UniFrac dissimilarity | 1.0144 | 0.181 | 0.428 |
| Unweighted UniFrac dissimilarity | 1.188 | 0.205 | 0.018* |

Number of permutations: 999
Signif. codes: 0.001 '***' 0.01 '**' 0.05 '*' 0.1 ' ' 1

**B)**

| Dist1 | Dist 2 | Mantel_R | P-value |
|---|---|---|---|
| Bray-Curtis dissimilarity | Weighted UniFrac dissimilarity | 0.908 | 0.001*** |
| Bray-Curtis dissimilarity | Unweighted UniFrac dissimilarity | 0.282 | 0.016* |
| Weighted UniFrac dissimilarity | Unweighted UniFrac dissimilarity | 0.242 | 0.013* |

Number of permutations: 999
Signif. codes: 0.001 '***' 0.01 '**' 0.05 '*' 0.1 ' ' 1

**Supplementary Table S5** Results of differential abundance analyses, taxonomic affiliation and maximal relative abundances of ASVs that changed significantly in response to high diatom vs. high cyanobacteria deposition. Abbreviations: log2FC, log2 fold change according to the differential abundance analysis using the DESeq2 package (log2FC<0: ASV abundance higher under high diatom deposition; log2FC >0: ASV abundance higher under high cyanobacteria deposition); lfcSE, standard error of log2-fold change; padj, significance P values were adjusted using the Benjamini and Hochberg method of the DESeq2 package; Max%, maximal relative abundance of the given ASV; Micro_ID, the microcosm in which the maximal relative abundance was detected. The ASV ID and log2FC in red (blue) indicate ASV enrichment in response to high diatom (cyanobacteria) deposition.

| ASV ID | FC | padj | Phylum | Class | Order | Family | Genus | Max% | Micro_ID |
|---|---|---|---|---|---|---|---|---|---|
| 16S_364 | -7.59 | 1.48E-05 | *Proteobacteria* | *Gammaproteobacteria* | *Nitrosococcales* | *Methylophagaceae* | Unclassified | 0.23 | 100D |
| 16S_329 | -7.52 | 1.48E-05 | *Proteobacteria* | *Gammaproteobacteria* | *Nitrosococcales* | *Methylophagaceae* | *Marine Methylotrophic Group 3* | 0.28 | 100D |
| 16S_374 | -7.24 | 2.44E-05 | *Proteobacteria* | *Gammaproteobacteria* | *Nitrosococcales* | *Methylophagaceae* | *Marine Methylotrophic Group 3* | 0.23 | 100D |
| 16S_390 | -7.23 | 2.12E-05 | *Proteobacteria* | *Gammaproteobacteria* | *Nitrosococcales* | *Methylophagaceae* | *Marine Methylotrophic Group 3* | 0.23 | 100D |
| 16S_274 | -7.02 | 1.13E-04 | *Proteobacteria* | *Gammaproteobacteria* | *Nitrosococcales* | *Methylophagaceae* | *Marine Methylotrophic Group 3* | 0.36 | 100D |
| 16S_354 | -6.61 | 5.06E-04 | *Proteobacteria* | *Gammaproteobacteria* | *Nitrosococcales* | *Methylophagaceae* | *Marine Methylotrophic Group 3* | 0.25 | 100D |
| 16S_1272 | -6.38 | 7.46E-03 | *Proteobacteria* | *Gammaproteobacteria* | *Pseudomonadales* | *Pseudomonadaceae* | *Pseudomonas* | 0.05 | 50D_50C |
| 16S_1312 | -6.37 | 1.59E-02 | *Proteobacteria* | *Gammaproteobacteria* | *Pseudomonadales* | *Pseudomonadaceae* | *Pseudomonas* | 0.04 | 50D_50C |
| 16S_359 | -6.28 | 1.81E-03 | *Proteobacteria* | *Gammaproteobacteria* | *Nitrosococcales* | *Methylophagaceae* | *Marine Methylotrophic Group 3* | 0.25 | 100D |
| 16S_1269 | -6.14 | 1.22E-01 | *Proteobacteria* | *Gammaproteobacteria* | *Nitrosococcales* | *Methylophagaceae* | Unclassified | 0.04 | 80D_20C |
| 16S_1770 | -5.94 | 1.39E-01 | *Bacteroidetes* | *Bacteroidia* | *Flavobacteriales* | *Flavobacteriaceae* | *Flavobacterium* | 0.03 | 80D_20C |
| 16S_282 | -5.88 | 9.60E-03 | *Proteobacteria* | *Gammaproteobacteria* | *Nitrosococcales* | *Methylophagaceae* | Unclassified | 0.32 | 100D |
| 16S_1331 | -5.86 | 1.61E-01 | *Proteobacteria* | *Gammaproteobacteria* | *Nitrosococcales* | *Methylophagaceae* | Unclassified | 0.04 | 80D_20C |
| 16S_1223 | -5.80 | 8.23E-02 | *Proteobacteria* | *Gammaproteobacteria* | *Pseudomonadales* | *Pseudomonadaceae* | *Pseudomonas* | 0.02 | 50D_50C |
| 16S_2053 | -5.80 | 1.61E-01 | *Actinobacteria* | *Actinobacteria* | *Frankiales* | *Sporichthyaceae* | *hgcI clade* | 0.02 | 80D_20C |
| 16S_1622 | -5.61 | 9.88E-02 | *Proteobacteria* | *Gammaproteobacteria* | *Pseudomonadales* | *Pseudomonadaceae* | *Pseudomonas* | 0.02 | 100D |
| 16S_1865 | -5.60 | 9.88E-02 | *Proteobacteria* | *Gammaproteobacteria* | *Pseudomonadales* | *Pseudomonadaceae* | *Pseudomonas* | 0.02 | 80D_20C |
| 16S_21 | -1.79 | 3.81E-02 | *Proteobacteria* | *Gammaproteobacteria* | *Nitrosococcales* | *Methylophagaceae* | *Marine Methylotrophic Group 3* | 2.12 | 100D |
| 16S_19 | -1.77 | 3.81E-02 | *Proteobacteria* | *Gammaproteobacteria* | *Nitrosococcales* | *Methylophagaceae* | *Unclassified* | 2.74 | 100D |
| 16S_26 | -1.77 | 3.81E-02 | *Proteobacteria* | *Gammaproteobacteria* | *Nitrosococcales* | *Methylophagaceae* | *Marine Methylotrophic Group 3* | 1.98 | 100D |
| 16S_18 | -1.75 | 4.42E-02 | *Proteobacteria* | *Gammaproteobacteria* | *Nitrosococcales* | *Methylophagaceae* | *Marine Methylotrophic Group 3* | 2.79 | 100D |
| 16S_24 | -1.75 | 4.42E-02 | *Proteobacteria* | *Gammaproteobacteria* | *Nitrosococcales* | *Methylophagaceae* | *Marine Methylotrophic Group 3* | 1.93 | 100D |
| 16S_23 | -1.70 | 4.42E-02 | *Proteobacteria* | *Gammaproteobacteria* | *Nitrosococcales* | *Methylophagaceae* | *Marine Methylotrophic Group 3* | 1.68 | 100D |
| 16S_20 | -1.69 | 4.42E-02 | *Proteobacteria* | *Gammaproteobacteria* | *Nitrosococcales* | *Methylophagaceae* | *Unclassified* | 2.39 | 100D |
| 16S_17 | -1.67 | 6.18E-02 | *Proteobacteria* | *Gammaproteobacteria* | *Nitrosococcales* | *Methylophagaceae* | *Marine Methylotrophic Group 3* | 2.40 | 100D |

| ASV ID | FC | padj | Phylum | Class | Order | Family | Genus | Max% | Micro_ID |
|---|---|---|---|---|---|---|---|---|---|
| 16S_22 | -1.65 | 7.11E-02 | Proteobacteria | Gammaproteobacteria | Nitrosococcales | Methylophagaceae | Marine Methylotrophic Group 3 | 1.78 | 100D |
| 16S_25 | -1.64 | 6.46E-02 | Proteobacteria | Gammaproteobacteria | Nitrosococcales | Methylophagaceae | Marine Methylotrophic Group 3 | 1.63 | 100D |
| 16S_27 | -1.61 | 6.18E-02 | Proteobacteria | Gammaproteobacteria | Nitrosococcales | Methylophagaceae | Marine Methylotrophic Group 3 | 1.61 | 100D |
| 16S_59 | 2.08 | 3.56E-02 | Proteobacteria | Gammaproteobacteria | Oceanospirillales | Nitrincolaceae | Neptunomonas | 0.74 | 20D_80C |
| 16S_60 | 2.13 | 2.41E-02 | Proteobacteria | Gammaproteobacteria | Oceanospirillales | Nitrincolaceae | Unclassified | 0.71 | 20D_80C |
| 16S_37 | 2.15 | 2.32E-02 | Proteobacteria | Gammaproteobacteria | Oceanospirillales | Nitrincolaceae | Unclassified | 1.03 | 50D_50C |
| 16S_38 | 2.15 | 1.83E-02 | Proteobacteria | Gammaproteobacteria | Oceanospirillales | Nitrincolaceae | Unclassified | 0.99 | 20D_80C |
| 16S_68 | 2.16 | 3.29E-02 | Proteobacteria | Gammaproteobacteria | Oceanospirillales | Nitrincolaceae | Unclassified | 0.66 | 50D_50C |
| 16S_69 | 2.16 | 2.58E-02 | Proteobacteria | Gammaproteobacteria | Oceanospirillales | Nitrincolaceae | Unclassified | 0.69 | 20D_80C |
| 16S_53 | 2.23 | 1.41E-02 | Proteobacteria | Gammaproteobacteria | Oceanospirillales | Nitrincolaceae | Unclassified | 0.80 | 20D_80C |
| 16S_51 | 2.26 | 1.41E-02 | Proteobacteria | Gammaproteobacteria | Oceanospirillales | Nitrincolaceae | Unclassified | 0.82 | 50D_50C |
| 16S_48 | 2.26 | 1.41E-02 | Proteobacteria | Gammaproteobacteria | Oceanospirillales | Nitrincolaceae | Unclassified | 0.87 | 20D_80C |
| 16S_34 | 2.27 | 1.59E-02 | Proteobacteria | Gammaproteobacteria | Oceanospirillales | Nitrincolaceae | Unclassified | 1.17 | 20D_80C |
| 16S_63 | 2.28 | 1.38E-02 | Proteobacteria | Gammaproteobacteria | Oceanospirillales | Nitrincolaceae | Unclassified | 0.77 | 20D_80C |
| 16S_35 | 2.28 | 1.41E-02 | Proteobacteria | Gammaproteobacteria | Oceanospirillales | Nitrincolaceae | Unclassified | 1.13 | 20D_80C |
| 16S_449 | 2.49 | 1.67E-01 | Proteobacteria | Gammaproteobacteria | Betaproteobacteriales | Burkholderiaceae | Unclassified | 0.18 | 20D_80C |
| 16S_304 | 2.62 | 7.50E-02 | Proteobacteria | Alphaproteobacteria | Rhodobacterales | Rhodobacteraceae | Pseudorhodobacter | 0.41 | 100C |
| 16S_206 | 2.67 | 1.55E-02 | Proteobacteria | Alphaproteobacteria | Rhodobacterales | Rhodobacteraceae | Pseudorhodobacter | 0.59 | 100C |
| 16S_231 | 2.67 | 4.22E-02 | Proteobacteria | Alphaproteobacteria | Rhodobacterales | Rhodobacteraceae | Pseudorhodobacter | 0.55 | 100C |
| 16S_416 | 2.69 | 1.17E-01 | Proteobacteria | Gammaproteobacteria | Betaproteobacteriales | Burkholderiaceae | Unclassified | 0.23 | 20D_80C |
| 16S_421 | 2.72 | 1.09E-01 | Proteobacteria | Gammaproteobacteria | Betaproteobacteriales | Burkholderiaceae | Unclassified | 0.21 | 20D_80C |
| 16S_341 | 2.74 | 1.03E-01 | Proteobacteria | Alphaproteobacteria | Rhodobacterales | Rhodobacteraceae | Pseudorhodobacter | 0.37 | 100C |
| 16S_302 | 2.74 | 5.48E-02 | Proteobacteria | Alphaproteobacteria | Rhodobacterales | Rhodobacteraceae | Pseudorhodobacter | 0.39 | 100C |
| 16S_327 | 2.76 | 1.00E-01 | Proteobacteria | Alphaproteobacteria | Rhodobacterales | Rhodobacteraceae | Pseudorhodobacter | 0.40 | 100C |
| 16S_276 | 2.81 | 9.55E-02 | Proteobacteria | Alphaproteobacteria | Rhodobacterales | Rhodobacteraceae | Pseudorhodobacter | 0.45 | 100C |
| 16S_334 | 2.81 | 9.80E-02 | Proteobacteria | Alphaproteobacteria | Rhodobacterales | Rhodobacteraceae | Pseudorhodobacter | 0.38 | 100C |
| 16S_298 | 2.81 | 9.86E-02 | Proteobacteria | Alphaproteobacteria | Rhodobacterales | Rhodobacteraceae | Pseudorhodobacter | 0.43 | 100C |
| 16S_204 | 2.84 | 8.96E-03 | Proteobacteria | Alphaproteobacteria | Rhodobacterales | Rhodobacteraceae | Pseudorhodobacter | 0.63 | 100C |
| 16S_460 | 2.86 | 1.24E-01 | Proteobacteria | Gammaproteobacteria | Betaproteobacteriales | Burkholderiaceae | Unclassified | 0.17 | 20D_80C |
| 16S_406 | 2.86 | 7.85E-02 | Proteobacteria | Gammaproteobacteria | Betaproteobacteriales | Burkholderiaceae | Unclassified | 0.22 | 20D_80C |
| 16S_465 | 2.90 | 1.15E-01 | Proteobacteria | Gammaproteobacteria | Betaproteobacteriales | Burkholderiaceae | Unclassified | 0.18 | 20D_80C |
| 16S_311 | 2.90 | 8.91E-02 | Proteobacteria | Alphaproteobacteria | Rhodobacterales | Rhodobacteraceae | Pseudorhodobacter | 0.44 | 100C |
| 16S_229 | 2.92 | 1.89E-02 | Proteobacteria | Alphaproteobacteria | Rhodobacterales | Rhodobacteraceae | Pseudorhodobacter | 0.57 | 100C |
| 16S_389 | 2.94 | 6.46E-02 | Proteobacteria | Gammaproteobacteria | Betaproteobacteriales | Burkholderiaceae | Unclassified | 0.25 | 20D_80C |
| 16S_520 | 3.05 | 1.32E-01 | Proteobacteria | Gammaproteobacteria | Betaproteobacteriales | Burkholderiaceae | Unclassified | 0.14 | 20D_80C |
| 16S_995 | 3.32 | 1.00E-01 | Proteobacteria | Gammaproteobacteria | Betaproteobacteriales | Burkholderiaceae | Unclassified | 0.03 | 100C |
| 16S_666 | 3.45 | 9.23E-02 | Proteobacteria | Gammaproteobacteria | Betaproteobacteriales | Burkholderiaceae | Unclassified | 0.07 | 50D_50C |
| 16S_950 | 3.67 | 9.12E-02 | Proteobacteria | Gammaproteobacteria | Betaproteobacteriales | Burkholderiaceae | Unclassified | 0.04 | 50D_50C |

| ASV ID | FC | padj | Phylum | Class | Order | Family | Genus | Max% | Micro_ID |
|---|---|---|---|---|---|---|---|---|---|
| 16S_125 | 3.99 | 2.68E-02 | Patescibacteria | Gracilibacteria | JGI 0000069-P22 | Unclassified | Unclassified | 0.93 | 100C |
| 16S_162 | 4.02 | 2.05E-02 | Patescibacteria | Gracilibacteria | JGI 0000069-P22 | Unclassified | Unclassified | 0.72 | 20D_80C |
| 16S_167 | 4.05 | 1.12E-02 | Patescibacteria | Gracilibacteria | JGI 0000069-P22 | Unclassified | Unclassified | 0.69 | 100C |
| 16S_147 | 4.10 | 1.89E-02 | Patescibacteria | Gracilibacteria | JGI 0000069-P22 | Unclassified | Unclassified | 0.79 | 20D_80C |
| 16S_156 | 4.12 | 1.89E-02 | Patescibacteria | Gracilibacteria | JGI 0000069-P22 | Unclassified | Unclassified | 0.76 | 20D_80C |
| 16S_117 | 4.12 | 2.05E-02 | Patescibacteria | Gracilibacteria | JGI 0000069-P22 | Unclassified | Unclassified | 0.98 | 20D_80C |
| 16S_112 | 4.19 | 1.74E-02 | Patescibacteria | Gracilibacteria | JGI 0000069-P22 | Unclassified | Unclassified | 1.04 | 20D_80C |
| 16S_152 | 4.20 | 9.49E-03 | Patescibacteria | Gracilibacteria | JGI 0000069-P22 | Unclassified | Unclassified | 0.77 | 20D_80C |
| 16S_172 | 4.20 | 1.50E-02 | Patescibacteria | Gracilibacteria | JGI 0000069-P22 | Unclassified | Unclassified | 0.67 | 20D_80C |
| 16S_178 | 4.21 | 1.55E-02 | Patescibacteria | Gracilibacteria | JGI 0000069-P22 | Unclassified | Unclassified | 0.65 | 20D_80C |
| 16S_836 | 4.21 | 1.41E-02 | Proteobacteria | Gammaproteobacteria | Betaproteobacteriales | Burkholderiaceae | Unclassified | 0.05 | 50D_50C |
| 16S_179 | 4.22 | 1.41E-02 | Patescibacteria | Gracilibacteria | JGI 0000069-P22 | Unclassified | Unclassified | 0.64 | 20D_80C |
| 16S_107 | 4.28 | 1.58E-02 | Patescibacteria | Gracilibacteria | JGI 0000069-P22 | Unclassified | Unclassified | 1.13 | 20D_80C |
| 16S_2099 | 5.91 | 1.66E-01 | Proteobacteria | Gammaproteobacteria | Betaproteobacteriales | Burkholderiaceae | Unclassified | 0.02 | 20D_80C |
| 16S_2029 | 5.92 | 1.72E-01 | Bacteroidetes | Bacteroidia | Flavobacteriales | Flavobacteriaceae | Flavobacterium | 0.03 | 100D |
| 16S_2409 | 6.07 | 1.36E-01 | Proteobacteria | Alphaproteobacteria | Caulobacterales | Hyphomonadaceae | Hyphomonas | 0.02 | 50D_50C |
| 16S_2687 | 6.11 | 1.30E-01 | Patescibacteria | Microgenomatia | Candidatus Pacebacteria | Unclassified | Unclassified | 0.03 | 100C |
| 16S_2242 | 6.11 | 6.46E-02 | Bacteroidetes | Bacteroidia | Flavobacteriales | Crocinitomicaceae | Unclassified | 0.02 | 20D_80C |
| 16S_1588 | 6.13 | 1.35E-01 | Proteobacteria | Alphaproteobacteria | Rhodobacterales | Rhodobacteraceae | Pseudorhodobacter | 0.02 | 100C |
| 16S_1824 | 6.14 | 1.36E-01 | Proteobacteria | Gammaproteobacteria | Betaproteobacteriales | Rhodocyclaceae | Unclassified | 0.01 | 100C |
| 16S_1360 | 6.38 | 1.12E-01 | Proteobacteria | Gammaproteobacteria | Betaproteobacteriales | Rhodocyclaceae | Unclassified | 0.01 | 100C |
| 16S_1933 | 6.39 | 1.10E-01 | Actinobacteria | Acidimicrobiia | Microtrichales | Ilumatobacteraceae | CL500-29 marine group | 0.03 | Control |
| 16S_2110 | 6.82 | 3.66E-02 | Proteobacteria | Alphaproteobacteria | Caulobacterales | Hyphomonadaceae | Hyphomonas | 0.02 | 50D_50C |
| 16S_1523 | 7.06 | 1.63E-04 | Bacteroidetes | Bacteroidia | Flavobacteriales | Crocinitomicaceae | Unclassified | 0.03 | 100C |
| 16S_1654 | 7.07 | 2.21E-02 | Patescibacteria | Parcubacteria | Candidatus Kaiserbacteria | Unclassified | Unclassified | 0.03 | 20D_80C |
| 16S_1900 | 7.25 | 5.87E-02 | Actinobacteria | Actinobacteria | Corynebacteriales | Unclassified | Unclassified | 0.03 | 20D_80C |
| 16S_1280 | 7.88 | 1.58E-02 | Patescibacteria | Gracilibacteria | JGI 0000069-P22 | Unclassified | Unclassified | 0.08 | 100C |
| 16S_1138 | 8.16 | 1.33E-02 | Patescibacteria | Gracilibacteria | JGI 0000069-P22 | Unclassified | Unclassified | 0.10 | 20D_80C |
| 16S_1169 | 8.21 | 1.33E-02 | Patescibacteria | Gracilibacteria | JGI 0000069-P22 | Unclassified | Unclassified | 0.12 | 20D_80C |
| 16S_1101 | 8.23 | 1.33E-02 | Patescibacteria | Gracilibacteria | JGI 0000069-P22 | Unclassified | Unclassified | 0.11 | 20D_80C |
| 16S_1181 | 8.35 | 1.14E-02 | Patescibacteria | Gracilibacteria | JGI 0000069-P22 | Unclassified | Unclassified | 0.12 | 20D_80C |
| 16S_1100 | 8.37 | 1.14E-02 | Patescibacteria | Gracilibacteria | JGI 0000069-P22 | Unclassified | Unclassified | 0.12 | 20D_80C |
| 16S_1037 | 8.43 | 1.12E-02 | Patescibacteria | Gracilibacteria | JGI 0000069-P22 | Unclassified | Unclassified | 0.13 | 20D_80C |
| 16S_945 | 8.59 | 1.12E-02 | Patescibacteria | Gracilibacteria | JGI 0000069-P22 | Unclassified | Unclassified | 0.15 | 20D_80C |
| 16S_879 | 8.65 | 1.05E-02 | Patescibacteria | Gracilibacteria | JGI 0000069-P22 | Unclassified | Unclassified | 0.15 | 20D_80C |
| 16S_897 | 8.72 | 1.04E-02 | Patescibacteria | Gracilibacteria | JGI 0000069-P22 | Unclassified | Unclassified | 0.15 | 20D_80C |
| 16S_857 | 8.73 | 1.05E-02 | Patescibacteria | Gracilibacteria | JGI 0000069-P22 | Unclassified | Unclassified | 0.16 | 20D_80C |

**Supplementary Table S6** Results of the phylogenetic clustering analysis demonstrating the clustering of diatom-favored taxa according to the net relatedness index (NRI) and the nearest taxon index (NTI). Standardized effect size scores (Z; difference between observed and expected values, divided by the SD of the expected values) are reported as means of all replicates per factor. The Z values are equivalent to negative NRI or NTI. Specifically, NRI or NTI greater than +2 indicates coexisting taxa within a community are more closely related than expected by chance (phylogenetic clustering). NRI or NTI less than -2 indicates coexisting taxa are more distantly related than expected by chance (phylogenetic overdispersion). A difference between the two metrices is expected when the clustering is shallow.

| | ntaxa | mpd.obs | mpd.rand.mean | mpd.rand.sd | mpd.obs.rank | mpd.obs.z | NRI | P-value | runs |
|---|---|---|---|---|---|---|---|---|---|
| Diatom-favored taxa | 28 | 0.150 | 0.604 | 0.044 | 1.000 | -10.407 | 10.407 | 0.001 | 999 |
| Cyano-favored taxa | 72 | 0.498 | 0.605 | 0.029 | 2.000 | -3.649 | 3.649 | 0.002 | 999 |

| | ntaxa | mpd.obs | mpd.rand.mean | mpd.rand.sd | mpd.obs.rank | mpd.obs.z | NTI | P-value | runs |
|---|---|---|---|---|---|---|---|---|---|
| Diatom-favored taxa | 28 | 0.043 | 0.205 | 0.036 | 1.000 | -4.445 | 4.445 | 0.001 | 999 |
| Cyano-favored taxa | 72 | 0.043 | 0.129 | 0.017 | 1.000 | -5.221 | 5.221 | 0.001 | 999 |

Abbreviations (based on Kembel et al., 2010):
ntaxa, number of taxa in community;
mpd.obs, observed mpd in community;
mpd. rand. mean, mean mpd in null communities;
mpd.rand.sd, standard deviation of mpd in null communities;
mpd. obs. rank, rank of observed mpd vs. null communities;
mpd. obs. z, Standardized effect size of mpd vs. null communities (= (mpd.obs - mpd.rand.mean)/ mpd.rand.sd, equivalent to -NRI);
P-value: quantile of observed mpd vs. null communities (= mpd.obs.rank / runs+ 1);
runs, number of randomizations.

**Supplementary Text** Correlation between relative and absolute abundance

Though we determined the responses of bacterial communities to POM addition using the relative abundance obtained from 16S rRNA amplicon sequencing, we also checked if the overall patterns were maintained if we used absolute abundance for analyses. For each ASV found in each sample, we calculated its 'estimated' absolute abundance by multiplying the 16S relative abundance with the total bacterial cell counts in that sample. We then run several analyses as follows:

1) **Linear regression**: In Props et al., (2017), the authors used Ordinary Least Squares linear regression to test the correlation between 16S relative abundance and absolute abundance for the OTUs surveyed. We thus applied the same approach to test if there was a correlation between 16S relative abundance and absolute abundance for each of the 100 ASVs whose abundance had significant changes across the POM resource gradient. We then performed linear regressions for each of the those 100 ASVs individually, using the 'lm' function in 'stats' package. We found that the relative and absolute abundances were significantly correlated for all 100 ASVs (e.g., lowest adjusted $R^2$=0.73739804 and $P$ <0.001; please see details in Supplementary Table S7). In addition, POM mixtures did not appear to alter total bacterial cell abundances in our microcosms on day 24, e.g., no significant difference in bacterial abundances between the treatments at the end of the experiment (Please see Supplementary information Fig. S4), thus likely diminishing the differences in responses determined using relative and absolute abundance data. Together with the linear regression tests, we are able to verify that for example, a cyanobacteria-preferred ASV increased in abundance relative to the overall community in high cyanobacteria POM treatments, would not have realized a decrease in overall cell density or biomass.

2) **Beta-diversity and PERMANOVA**: We compared community similarity based on absolute abundance data using Bray-Curtis dissimilarity matrix and then carried out a PERMANOVA to test the effects of POM addition on community variation. We found that the effects of POM addition on the absolute abundance was significant (PERMANOVA, pseudo-F=2.2594, $R^2$=0.32939, *P*=0.001; Supplementary Figure S7). The overall pattern of beta-diversity based on absolute abundance was similar to that based on relative abundance (Supplementary Figure S7).

3) **Mantel test and Procrustes test for matrix association**: The Mantel test provides a mean to test the association between distance matrices and has been widely used in ecological studies (e.g., Glassman and Martiny, 2018). Another permutation test based on a Procrustes statistic (PROTEST) was developed to compare multivariate data sets. The two tests have been reported for other ecological studies. We applied both tests to our dataset as they pertain to the model of matrix association and have slightly different statistical power. We found the associate matrices based on relative and absolute abundance data to be statistically indistinguishable by those two tests (correlation in a symmetric Procrustes rotation = 0.6926 and P-value=0.001 on 999 permutations; Mantel correlation = 0.4332 and P-value=0.001 on 999 permutations; Supplementary Table S8).

**Supplementary Figure S7** NMDS ordination displaying Beta-diversity based on absolute abundance and the result of PERMANOVA testing the effect of POM addition on community variation.

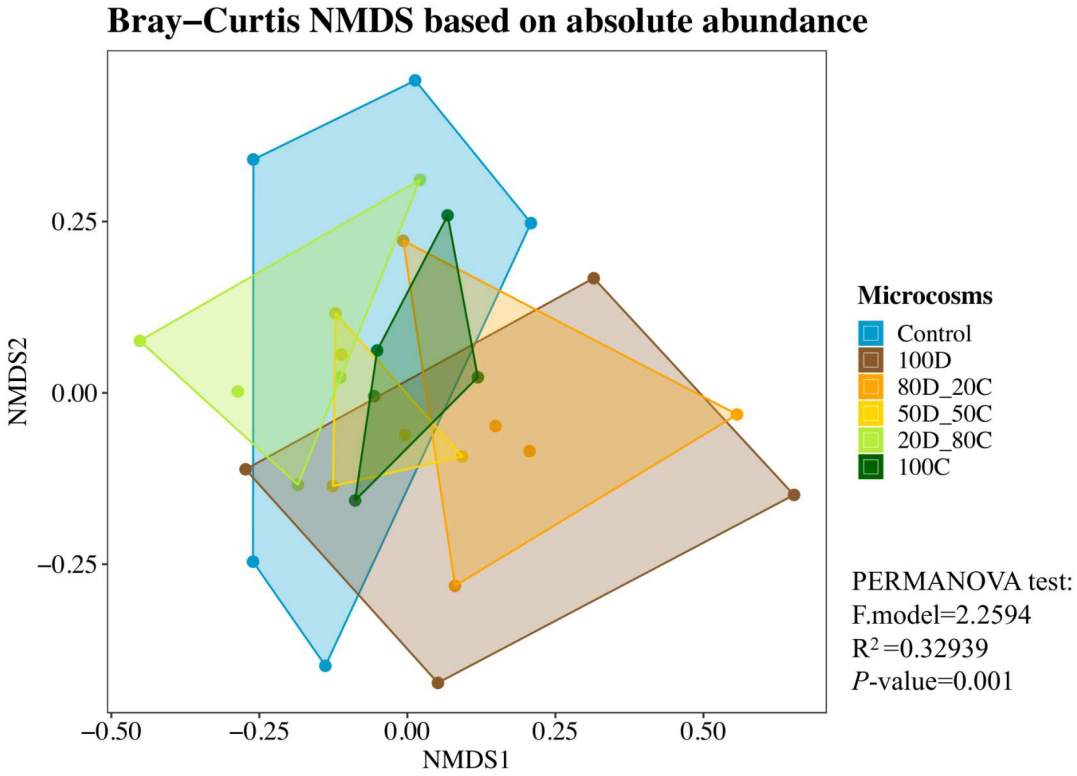

**Supplementary Table S7** The results of linear regressions testing the correlation between the relative and absolute abundances for each of the 100ASVs whose relative abundance significantly changed across the POM mixture gradient. $R^2$ value, a regression coefficient indicates correlation strength.

| ASV ID | $R^2$ | adj.$R^2$ | P-value |
|---|---|---|---|
| 16S_1037 | 0.94892638 | 0.94660485 | 8.32E-07 |
| 16S_107 | 0.93940704 | 0.93665281 | 7.66E-07 |
| 16S_1100 | 0.94761988 | 0.94523897 | 8.10E-07 |
| 16S_1101 | 0.94843632 | 0.94609252 | 7.89E-07 |
| 16S_112 | 0.93985187 | 0.93711786 | 7.64E-07 |
| 16S_1138 | 0.9477107 | 0.94533391 | 7.91E-07 |
| 16S_1169 | 0.95275159 | 0.95060393 | 8.54E-07 |
| 16S_117 | 0.93978323 | 0.93704611 | 7.58E-07 |
| 16S_1181 | 0.94786574 | 0.945496 | 8.23E-07 |
| 16S_1223 | 0.84842718 | 0.84153751 | 5.44E-07 |
| 16S_125 | 0.94027141 | 0.93755647 | 7.52E-07 |
| 16S_1269 | 0.8530078 | 0.84632634 | 7.05E-07 |
| 16S_1272 | 0.95645431 | 0.95447496 | 5.19E-07 |
| 16S_1280 | 0.9514497 | 0.94924287 | 7.59E-07 |
| 16S_1312 | 0.91086791 | 0.90681645 | 5.49E-07 |
| 16S_1331 | 0.89620437 | 0.89148638 | 8.20E-07 |
| 16S_1360 | 0.96712026 | 0.96562573 | 7.31E-07 |
| 16S_147 | 0.93943796 | 0.93668514 | 7.59E-07 |
| 16S_152 | 0.93985494 | 0.93712107 | 7.66E-07 |
| 16S_1523 | 0.84158128 | 0.83438043 | 6.48E-07 |

| ASV ID | $R^2$ | adj.$R^2$ | P-value |
|---|---|---|---|
| 16S_156 | 0.94114445 | 0.9384692 | 7.56E-07 |
| 16S_1588 | 0.9541218 | 0.95203643 | 7.60E-07 |
| 16S_162 | 0.93875283 | 0.93596887 | 7.65E-07 |
| 16S_1622 | 0.86290448 | 0.85667287 | 4.90E-07 |
| 16S_1654 | 0.94852105 | 0.9461811 | 7.20E-07 |
| 16S_167 | 0.94018165 | 0.93746264 | 7.58E-07 |
| 16S_17 | 0.87179796 | 0.86597059 | 5.30E-07 |
| 16S_172 | 0.93948771 | 0.93673715 | 7.60E-07 |
| 16S_1770 | 0.89201149 | 0.88710292 | 7.04E-07 |
| 16S_178 | 0.94039873 | 0.93768958 | 7.59E-07 |
| 16S_179 | 0.93933675 | 0.93657933 | 7.69E-07 |
| 16S_18 | 0.90064074 | 0.89612441 | 5.38E-07 |
| 16S_1824 | 0.97297661 | 0.97174828 | 7.20E-07 |
| 16S_1865 | 0.83713881 | 0.82973603 | 5.36E-07 |
| 16S_19 | 0.89805162 | 0.8934176 | 5.39E-07 |
| 16S_1900 | 0.97284342 | 0.97160903 | 7.49E-07 |
| 16S_1933 | 0.91385698 | 0.90994139 | 9.00E-07 |
| 16S_20 | 0.87484773 | 0.86915899 | 5.33E-07 |
| 16S_2029 | 0.91212951 | 0.90813539 | 6.15E-07 |
| 16S_204 | 0.90778845 | 0.90359702 | 9.93E-07 |

| ASV ID | $R^2$ | adj.$R^2$ | P-value |
|---|---|---|---|
| 16S_2053 | 0.83818322 | 0.83082791 | 5.91E-07 |
| 16S_206 | 0.90288829 | 0.89847413 | 9.88E-07 |
| 16S_2099 | 0.91415632 | 0.91025433 | 7.82E-07 |
| 16S_21 | 0.90260988 | 0.89818305 | 5.40E-07 |
| 16S_2110 | 0.89422545 | 0.88941752 | 5.97E-07 |
| 16S_22 | 0.86884049 | 0.8628787 | 5.31E-07 |
| 16S_2242 | 0.891184 | 0.88623782 | 6.97E-07 |
| 16S_229 | 0.91105861 | 0.90701581 | 1.00E-06 |
| 16S_23 | 0.87416473 | 0.86844495 | 5.30E-07 |
| 16S_231 | 0.90048394 | 0.89596049 | 9.83E-07 |
| 16S_24 | 0.89853736 | 0.89392543 | 5.39E-07 |
| 16S_2409 | 0.93013187 | 0.92695604 | 5.78E-07 |
| 16S_25 | 0.86648718 | 0.86041842 | 5.35E-07 |
| 16S_26 | 0.91082656 | 0.90677322 | 5.41E-07 |
| 16S_2687 | 0.98185825 | 0.98103363 | 1.11E-06 |
| 16S_27 | 0.88085268 | 0.87543689 | 5.32E-07 |
| 16S_274 | 0.97647226 | 0.97540282 | 4.74E-07 |
| 16S_276 | 0.8879681 | 0.88287574 | 9.55E-07 |
| 16S_282 | 0.97385051 | 0.97266189 | 4.81E-07 |
| 16S_298 | 0.90446027 | 0.90011756 | 9.86E-07 |

| ASV ID | $R^2$ | adj.$R^2$ | P-value |
|---|---|---|---|
| 16S_302 | 0.89374235 | 0.88891245 | 9.68E-07 |
| 16S_304 | 0.89836002 | 0.89374002 | 9.82E-07 |
| 16S_311 | 0.91119416 | 0.90715753 | 9.98E-07 |
| 16S_327 | 0.8964482 | 0.8917413 | 9.72E-07 |
| 16S_329 | 0.97505214 | 0.97391814 | 4.99E-07 |
| 16S_334 | 0.90025553 | 0.89572169 | 9.72E-07 |
| 16S_34 | 0.75116956 | 0.73985909 | 6.42E-07 |
| 16S_341 | 0.90413867 | 0.89978133 | 9.83E-07 |
| 16S_35 | 0.75341171 | 0.74220315 | 6.29E-07 |
| 16S_354 | 0.97486332 | 0.97372075 | 4.83E-07 |
| 16S_359 | 0.97498285 | 0.97384571 | 4.85E-07 |
| 16S_364 | 0.97402571 | 0.97284506 | 4.93E-07 |
| 16S_37 | 0.74881552 | 0.73739804 | 6.40E-07 |
| 16S_374 | 0.97422276 | 0.97305107 | 5.00E-07 |
| 16S_38 | 0.7509689 | 0.73964931 | 6.26E-07 |
| 16S_389 | 0.94398894 | 0.94144299 | 9.44E-07 |
| 16S_390 | 0.97658486 | 0.97552054 | 4.77E-07 |
| 16S_406 | 0.93819901 | 0.93538988 | 9.50E-07 |
| 16S_416 | 0.9465839 | 0.94415589 | 9.42E-07 |
| 16S_421 | 0.95581573 | 0.95380735 | 9.59E-07 |

| ASV ID | $R^2$ | adj.$R^2$ | P-value |
|---|---|---|---|
| 16S_449 | 0.9392476 | 0.93648612 | 9.34E-07 |
| 16S_460 | 0.94923488 | 0.94692737 | 9.56E-07 |
| 16S_465 | 0.95796141 | 0.95605057 | 9.59E-07 |
| 16S_48 | 0.75852021 | 0.74754386 | 6.35E-07 |
| 16S_51 | 0.74604436 | 0.73450092 | 6.28E-07 |
| 16S_520 | 0.94739115 | 0.94499984 | 9.26E-07 |
| 16S_53 | 0.75311635 | 0.74189437 | 6.21E-07 |
| 16S_59 | 0.74967351 | 0.73829503 | 6.18E-07 |
| 16S_60 | 0.75041351 | 0.73906867 | 6.12E-07 |
| 16S_63 | 0.75674269 | 0.74568554 | 6.09E-07 |
| 16S_666 | 0.8665747 | 0.86050991 | 8.61E-07 |
| 16S_68 | 0.75111627 | 0.73980337 | 6.27E-07 |
| 16S_69 | 0.75490166 | 0.74376083 | 6.33E-07 |
| 16S_836 | 0.81406416 | 0.80561253 | 6.75E-07 |
| 16S_857 | 0.94849199 | 0.94615072 | 7.92E-07 |
| 16S_879 | 0.94783267 | 0.94546143 | 8.05E-07 |
| 16S_897 | 0.94742158 | 0.94503165 | 7.93E-07 |
| 16S_945 | 0.94840065 | 0.94605522 | 7.98E-07 |
| 16S_950 | 0.88201767 | 0.87665484 | 7.97E-07 |
| 16S_995 | 0.86368279 | 0.85748655 | 8.12E-07 |

**Supplementary Table S8** The results of PROTEST and Mantel tests illustrating association of beta-diversity matrices measured in terms of relative and absolute abundances.

| | Mantel test | | PROTEST | |
|---|---|---|---|---|
| | $R^2$ | P-value | $R^2$ | P-value |
| relative vs. absolute Beta-diversity | 0.4332 | 0.001 | 0.6926 | 0.001 |

Number of permutations: 999

**Supplementary references**:


Kembel SW, Cowan PD, Helmus MR, Cornwell WK, Morlon H, Ackerly DD et al. (2010). Picante: R tools for integrating phylogenies and ecology. Bioinformatics 26: 1463-1464.

Props, R., Kerckhof, F; Rubbens, P., Vrieze J., Sanabria, E.H., Waegeman, W et al., (2017). Absolute quantification of microbial taxon abundances. *ISME* 11: 584-587.

Glassman, S.I., Martiny, J.B.H. (2018). Broadscale ecological patterns are robust to use of exact sequence variants versus operational taxonomic units. *mSphere* 3: e00148-18.